CHEMISTRY
A EUROPEAN JOURNAL

DOI: 10.1002/chem.200800976

Valence-State Analysis through Spectroelectrochemistry in a Series of Quinonoid-Bridged Diruthenium Complexes $[(acac)_2Ru(\mu\text{-}L)Ru(acac)_2]^n$ ($n = +2, +1, 0, -1, -2$)

Sandeep Ghumaan,[a] Biprajit Sarkar,[b] Somnath Maji,[a] Vedavati G. Puranik,[e] Jan Fiedler,[c] Francisco A. Urbanos,[d] Reyes Jimenez-Aparicio,*[d] Wolfgang Kaim,*[b] and Goutam Kumar Lahiri*[a]

Abstract: The quinonoid ligand-bridged diruthenium compounds $[(acac)_2Ru(\mu\text{-}L^{2-})Ru(acac)_2]$ ($acac^- =$ acetylacetonato = 2,4-pentanedionato; $L^{2-} =$ 2,5-dioxido-1,4-benzoquinone, **1**; 3,6-dichloro-2,5-dioxido-1,4-benzoquinone, **2**; 5,8-dioxido-1,4-naphthoquinone, **3**; 2,3-dichloro-5,8-dioxido-1,4-naphthoquinone, **4**; 1,5-dioxido-9,10-anthraquinone, **5**; and 1,5-diimido-9,10-anthraquinone, **6**) were prepared and characterized analytically. The crystal structure analysis of **5** in the *rac* configuration reveals two tris(2,4-pentanedionato)ruthenium moieties with an extended anthracenedione-derived bis(ketoenolate) π-conjugated bridging ligand. The weakly antiferromagnetically coupled $\{Ru^{III}(\mu\text{-}L^{2-})Ru^{III}\}$ configuration in **1**–**6** exhibits complicated overall magnetic and EPR responses. The simultaneous presence of highly redox-active quinonoid-bridging ligands and of two ruthenium centers capable of adopting the oxidation states +2, +3, and +4 creates a large variety of possible oxidation state combinations. Accordingly, the complexes **1**–**6** exhibit two reversible one-electron oxidation steps and at least two reversible reduction processes. Shifts to positive potentials were observed on introduction of Cl substituents (**1**→**2**, **3**→**4**) or through replacement of NH by O (**6**→**5**). The ligand-to-metal charge transfer (LMCT) absorptions in the visible region of the neutral molecules become more intense and shifted to lower energies on stepwise reduction with two electrons. On oxidation, the *para*-substituted systems **1**–**4** exhibit monocation intermediates with intervalence charge transfer (IVCT) transitions of $Ru^{III}Ru^{IV}$ mixed-valent species. In contrast, the differently substituted systems **5** and **6** show no such near infrared (NIR) absorption. While the first reduction steps are thus assigned to largely ligand-centered processes, the oxidation appears to involve metal–ligand delocalized molecular orbitals with variable degrees of mixing.

Keywords: magnetic properties · quinones · ruthenium · spectroelectrochemistry · structure elucidation · valence-state distributions

[a] Dr. S. Ghumaan, S. Maji, Prof. Dr. G. K. Lahiri
Department of Chemistry, Indian Institute of Technology
Bombay, Powai, Mumbai-400076 (India)
Fax: (+91) 022-2572-3480
E-mail: lahiri@chem.iitb.ac.in

[b] Dr. B. Sarkar, Prof. Dr. W. Kaim
Institut für Anorganische Chemie, Universität Stuttgart
Pfaffenwaldring 55, 70550 Stuttgart (Germany)
Fax: (+49) 711-685-64165
E-mail: kaim@iac.uni-stuttgart.de

[c] Dr. J. Fiedler
J. Heyrovský Institute of Physical Chemistry
Academy of Sciences of the Czech Republic, Dolejškova 3, 18223
Prague (Czech Republic)

[d] Dr. F. A. Urbanos, Prof. Dr. R. Jimenez-Aparicio
Departamento de Química Inorgánica
Facultad de Ciencias Químicas, Universidad Complutense
Ciudad Universitaria, 28040-Madrid (Spain)
Fax: (+34) 91-394-4352
E-mail: reyesja@quim.ucm.es

[e] Dr. V. G. Puranik
Center for Materials Characterization
National Chemical Laboratory, Pune-411008 (India)

Supporting information for this article is available on the WWW under http://dx.doi.org/10.1002/chem.200800976.

Introduction

Bridging ligand mediated electronic coupling in mixed-valent polynuclear metal complexes constitutes the basis for intramolecular electron-transfer processes that have applications in designing molecular electronic devices[1] and in biochemical processes.[2] In this context, ruthenium compounds form the largest group of the mixed-valent systems as they undergo facile electron-transfer processes between the valence states of Ru^{II}, Ru^{III}, and Ru^{IV}. Thus, there have been continuous research efforts towards the development of new classes of polynuclear ruthenium complexes with the perspective of variable electronic and conformational effects from the bridging and ancillary ligands on the extent of coupling.[3] Recent experimental and theoretical studies with novel molecular frameworks have facilitated the emergence of 1) hybrid class II–class III systems,[4] in addition to the classical Robin and Day definitions of class II and class III mixed-valent species;[5] 2) large electrochemical coupling with comproportionation constants $K_c > 10^{10}$ in the $Ru^{II}Ru^{III}$ state, yet without detectable intervalence charge transfer (IVCT) transitions in the near infrared (NIR) region;[6] 3) the isolation of antiferromagnetically coupled diamagnetic radical-bridged mixed-valent species;[7] and 4) the detection of distinct IVCT transitions in the NIR region for the less common Ru^{III}/Ru^{IV} (d^4/d^5) mixed-valent state.[8]

The present work originates from our recent approach of introducing redox noninnocent quinonoid bridging ligands into diruthenium complexes.[9] This can introduce additional challenging features for the assignment of metal-, ligand-, or mixed metal–ligand-based frontier orbitals in the associated electron-transfer processes.[10] Thus, a group of six diruthenium complexes $[\{(acac)_2Ru\}_2(\mu\text{-}L)]$ ($acac^- =$ acetylacetonato = 2,4-pentanedionato) containing quinonoid bridging units of varying character and size were studied (**1**–**6**).

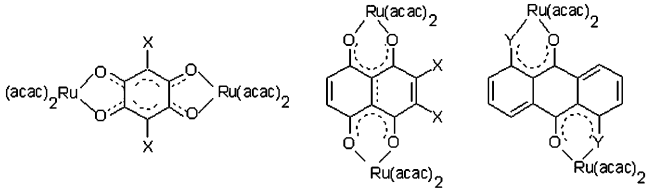

X = H **1** X = H **3** Y = O **5**

X = Cl **2** X = Cl **4** Y = NH **6**

Ortho- and *para*-quinones are heavily investigated organic compounds. Their characteristically low-lying unoccupied molecular orbitals can be occupied stepwise to result in corresponding three-component redox systems. The relevance of quinones ranges from naturally occurring substances, such as vitamins,[11] melanins, neurotransmitter metabolites,[12] electron-transport components,[13] or quinoproteins[14] and drugs (e.g., antiinfective[15] or cytostatic[16]) through analytical, electrochemical or color reagents[17] and optically interesting materials[18] to synthetic organic and industrial chemicals (anthraquinone dyes,[19] AO = alkylanthraquinone oxidation process of H_2O_2 production[20]). The conjugated nonaromatic π system of quinones is fascinating, especially when coupled with deprotonable OH functions and when incorporated in condensed, unsaturated ring systems. Coordination of metal ions within five- or six-membered chelating rings is a further option;[21,22] however, *p*-quinones have been much less studied[21] than the apparently better suited *ortho* analogues.[22]

In this work we present three kinds of quinone systems with different modes of π delocalization, but double metal-chelation potential towards the potentially redox-active $[Ru(acac)_2]^n$ ($n = +1, +2$ or 0, $acac^- = 2,4$-pentanedionato).

Two $[Ru(acac)_2]$ complex fragments were bridged in each case by L^-: 2,5-dioxido-1,4-benzoquinones (**1** and **2**), 5,8-dioxido-1,4-naphthoquinones (**3** and **4**) or 1,5-dioxido- or 1,5-diimido-9,10-anthraquinones (**5** and **6**). Chloride acceptors were introduced (in **2** and **4**) in order to investigate substituent effects; the metal coordination involves five-membered chelating rings for **1** and **2**, but six-membered 2,4-pentanedionato-type chelating rings for complexes **3**–**6.** The capability of the redox-active bridging ligands to undergo stepwise one-electron transfer as illustrated (see Scheme 1) leads to aromatic polyanions on reduction.

Like the corresponding dinuclear complex **7** of the quinizarine dianion (1,4-dioxidoanthraquinone),[23] the isomeric **5** and the NH analogue **6** exhibit partial π conjugation within the tricyclic ring system, and the similarity between **3** and **7** is evident.

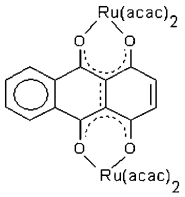

7

The preferential choice of σ-donating $acac^-$ as ancillary ligands in **1**–**6** facilitates the stabilization of the metal ions in the Ru^{III} state, which extends the possibility of 1) generating hitherto relatively little explored mixed-valent $Ru^{III}Ru^{IV}$ intermediate states and 2) allowing for magnetic exchange between two paramagnetic Ru^{III} centers in **1**–**6**. So far, only a limited number of dinuclear ruthenium complexes with such ligands have been reported: containing pyridine,[24] 2,2′-bipyridine,[25] 1,10-phenanthroline,[24] triphenylphosphine,[24] 2-(2′-pyridyl)quinoxaline,[26] and $acac^-$[27] as ancillary ligands with the 2,5-dioxido-1,4-benzoquinone bridge ($\mathbf{L1}^{2-}$), and containing NH_3 as ancillary ligands with the 2,5-dioxido-3,6-dichloro-1,4-benzoquinone ($\mathbf{L2}^{2-}$) bridge.[28] In the case of 5,8-dioxido-1,4-naphthoquinone ($\mathbf{L3}^{2-}$) and 1,5-dioxido-9,10-anthraquinone ($\mathbf{L5}^{2-}$), two complexes for each have been reported with the ancillary ligands pap[29] and bpy,[30,16b] respectively (pap = 2-phenylazopyridine, bpy = bipyridine). However, an appreciable number of dinuclear complexes of the ligands L^{2-} with other metal ions are known.[31]

Herein, we describe the synthesis of **1**–**6**, the crystal structure of the *rac* isomer of **5**, and the valence-state analysis of the complexes $[(acac)_2Ru(\mu\text{-}L)Ru(acac)_2]^{n+}$ in the accessible oxidized and reduced forms ($n = +2, +1, 0, -1, -2$). Susceptibility and EPR measurements as well as electrochemi-

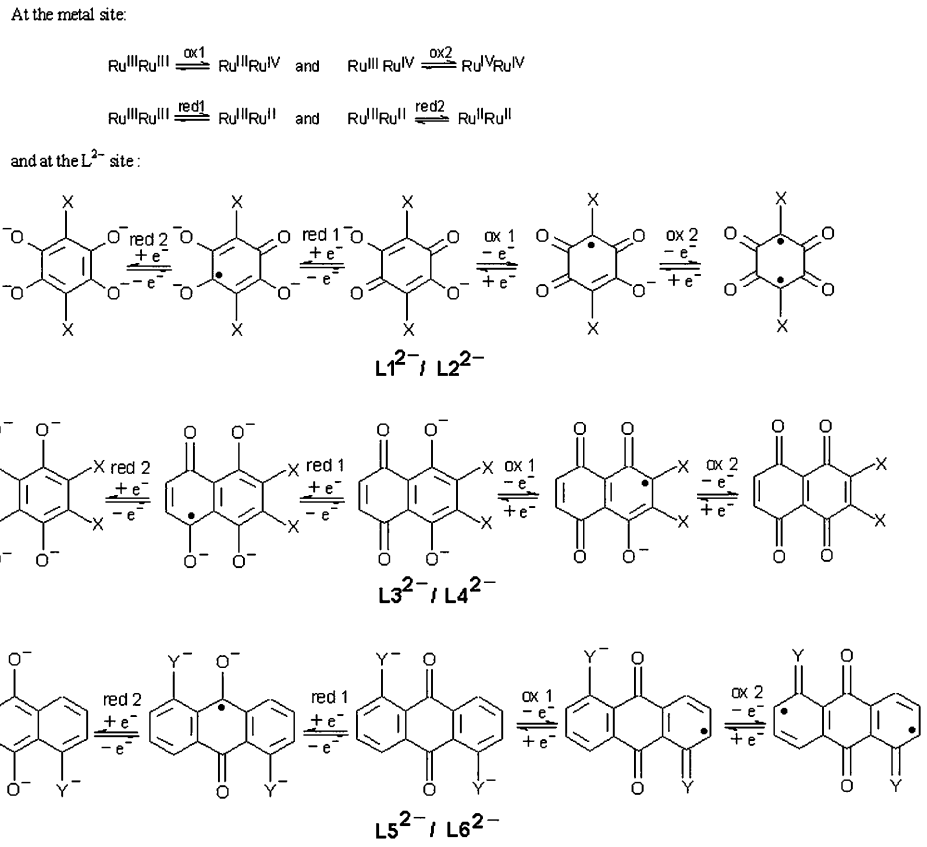

Scheme 1.

cal and spectroelectrochemical studies were undertaken for the systems **1**–**6**.

Results and Discussion

Synthesis and characterization of 1–6: The complexes **1**–**6** were prepared through the reaction of $[Ru(acac)_2(CH_3CN)_2]$ with the corresponding dihydroxy (H_2**L1**–H_2**L5**) or diamino ligand (H_2**L6**) in the presence of NEt_3 (Et = ethyl) as a base under aerobic conditions, followed by chromatographic purification using a silica gel column. The apparent ruthenium(II) to ruthenium(III) oxidation was facilitated by the admission of air. The presence of σ-donating $acac^-$ in **1**–**6** stabilizes the paramagnetic +3 oxidation state under aerobic reaction conditions as observed for many other $Ru(acac)_2$ derivatives.[32] The suggested chelating coordination involving the carbonyl functions in an electron-delocalized arrangement is supported by infrared (IR) vibrational spectroscopy. The $\nu_{C=O}$ bands from the coordinated ligands could not be found above 1600 cm^{-1} in the complexes **1**–**6**. The NH stretching band of coordinated $\mathbf{L6}^{2-}$ in **6** appears at 3307 cm^{-1}.

The electrically neutral complexes **1**–**6** exhibit satisfactory microanalytical data (see Experimental Section). The positive ion electrospray mass spectra are shown in Figure 1, which correspond to the respective molecular ion signals of $[\mathbf{1}]^+$–$[\mathbf{6}]^+$ (Table 1).

Although the reactions could be expected to yield mixtures of *rac* (C_2 symmetry, ΔΔ/ΛΛ) and *meso* (C_i symmetry, ΔΛ) species,[33] the preparatory TLC experiments suggested the presence of only one isomer in each case. Compounds **1**, **2**, **5**, and **6** exhibit reasonably resolved ^{1}H NMR spectra in $CDCl_3$ with a wide range of chemical shifts due to paramagnetic contact interactions (Figure 2, see Experimental Section).[3v,34,35] The ^{1}H NMR spectra of the complexes **3** and **4** were too broad and complicated to be analyzed. The NMR spectra of **1**, **2**, and **6** in $CDCl_3$ exhibit signals corresponding to half of the molecules, indicating formation of only the *meso* isomers. In contrast, **5** exhibits eight methyl and four CH proton resonances corresponding to four nonequivalent acac ligands, in addition to six "aromatic" protons (Figure 2, Experimental Section), as expected for a molecule of the *rac* isomers.

The crystal structure analysis of **5** confirms the crystallization of the *rac* isomer. The molecular structure in the crystal of **5** is shown in Figure 3. Crystallographic parameters and selected bond lengths and angles are given in Table 2 and Table 3.

The ruthenium ions are bonded to $\mathbf{L5}^{2-}$ through the oxygen donor centers in the π-conjugated "acac" mode at each end, leading to six-membered chelating rings. The

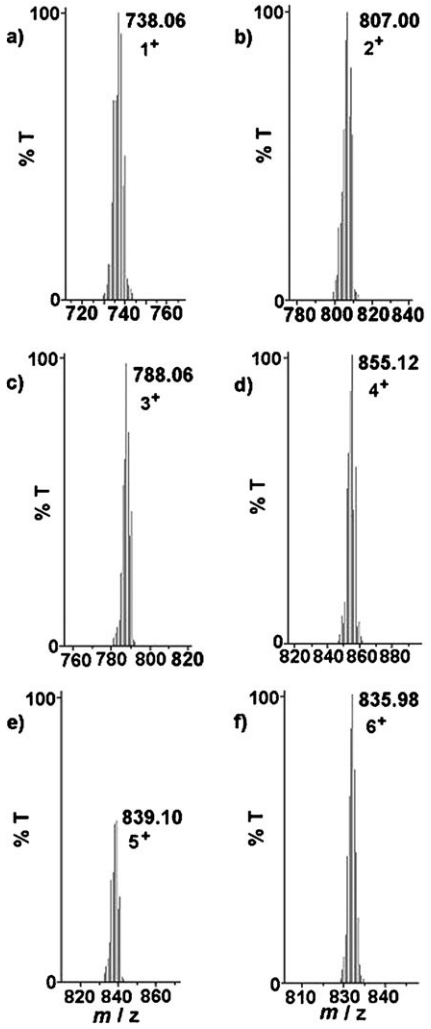

Figure 1. Electrospray mass spectra of a) **1**, b) **2**, c) **3**, d) **4**, e) **5** and f) **6** in CH_3CN.

Table 1. Mass spectral data.[a]

Complex	*m*/z (obsd)	Correspondence	*m*/*z* (calcd)
1	738.06	$[\mathbf{1}]^+$	737.98
	639.00	$[\mathbf{1}-\text{acac}]^+$	638.94
2	807.00	$[\mathbf{2}]^+$	805.90
	705.94	$[\mathbf{2}-\text{acac}]^+$	706.85
3	788.06	$[\mathbf{3}]^+$	787.99
	688.99	$[\mathbf{3}-\text{acac}]^+$	688.95
4	855.12	$[\mathbf{4}]^+$	855.92
5	839.10	$[\mathbf{5}]^+$	838.01
	738.04	$[\mathbf{5}-\text{acac}]^+$	738.97
6	835.98	$[\mathbf{6}]^+$	836.04

[a] In acetonitrile.

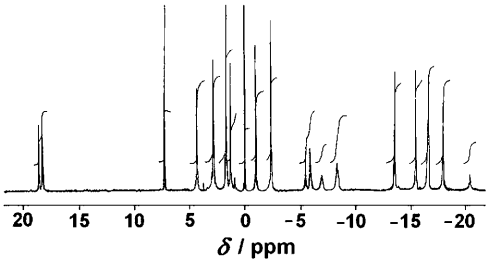

Figure 2. ^{1}H NMR spectrum of **5** in $CDCl_3$.

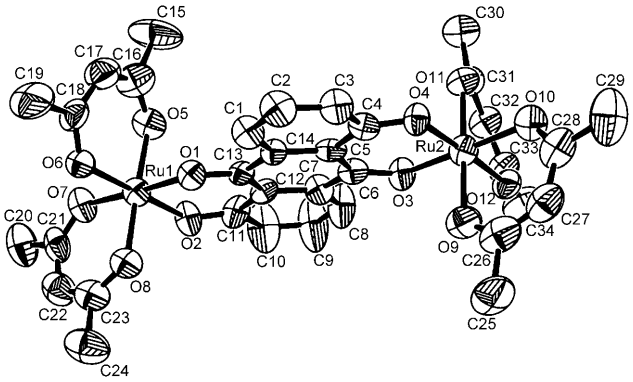

Figure 3. ORTEP diagram of **5**. Ellipsoids are drawn at the 50% probability level.

Table 2. Crystallographic data for **5**·0.25 H_2O.

formula	$C_{34}H_{34}O_{12.25}Ru_2$
M_r	840.75
crystal size [mm]	0.30×0.20×0.15
crystal system	monoclinic
space group	*C2/c*
a [Å]	28.988(9)
b [Å]	8.110(3)
c [Å]	30.896(10)
β [°]	108.368(5)
V [Å^3]	6893(4)
Z	8
F(000)	3392
μ [mm^{-1}]	0.939
T [K]	293(2)
hkl range	−31 to 31, −8 to 8, −33 to 33
ρ_{calcd} [g cm^{-3}]	1.620
2θ range [°]	4.66–45
reflns collected	27579
unique reflns [R_{int}]	4499 [0.1046]
data/restraints/parameters	4499/0/446
*R*1 [$I>2\sigma(I)$]	0.0886
*wR*2 [all data]	0.2263
goodness-of-fit	1.171
residual electron density [e Å^{-3}]	1.672, −1.366

metal ions are displaced by only 2.8° from the mean plane of the planar ligand bridge. Each RuO_6 chromophore is in a slightly distorted octahedral arrangement, as can be seen from the angles subtended at the metal ions (Table 3). The C–O distances pertaining to the bridging ligand are about 1.27 Å, which is in between the standard single (1.34 Å) and double (1.22 Å) bond C–O lengths.[36] The intraligand distances are given at the bottom of Table 3 and are compatible with the single/double-bond arrangement. Along with the Ru–O bond lengths of about 1.97 Å, this confirms the π-delocalized state of the keto–enolate forms in the ligand $\mathbf{L5}^{2-}$ of **5**.[3x,37] The Ru^{III}–O(acac) distances (average

Table 3. Selected bond lengths [Å] and angles [°] for **5**·0.25 H_2O.

Bond lengths		Bond angles	
Ru1–O2	1.968(7)	O2-Ru1-O1	91.5(3)
Ru1–O1	1.969(7)	O2-Ru1-O5	87.6(3)
Ru1–O5	1.972(8)	O1-Ru1-O5	87.7(3)
Ru1–O8	1.994(8)	O1-Ru1-O8	89.7(3)
Ru1–O6	1.997(7)	O2-Ru1-O8	92.0(3)
Ru1–O7	1.999(8)	O5-Ru1-O8	177.3(3)
Ru2–O3	1.964(7)	O2-Ru1-O6	179.2(3)
Ru2–O4	1.977(7)	O1-Ru1-O6	89.2(3)
Ru2–O9	1.992(9)	O5-Ru1-O6	92.1(3)
Ru2–O10	2.004(8)	O8-Ru1-O6	88.3(3)
Ru2–O11	2.006(8)	O2-Ru1-O7	90.1(3)
Ru2–O12	2.007(8)	O1-Ru1-O7	177.3(3)
O1–C13	1.271(11)	O5-Ru1-O7	90.2(3)
O2–C11	1.280(13)	O8-Ru1-O7	92.5(3)
O3–C6	1.267(12)	O6-Ru1-O7	89.2(3)
O4–C4	1.283(12)	O3-Ru2-O4	92.7(3)
O5–C16	1.272(16)	O3-Ru2-O9	89.5(4)
O6–C18	1.241(14)	O4-Ru2-O9	89.0(3)
O7–C21	1.243(14)	O3-Ru2-O10	177.0(3)
O8–C23	1.246(14)	O4-Ru2-O10	89.0(3)
O9–C26	1.303(18)	O9-Ru2-O10	93.0(4)
O10–C28	1.252(15)	O3-Ru2-O11	89.8(3)
O11–C31	1.308(12)	O4-Ru2-O11	91.3(3)
O12–C33	1.283(14)	O9-Ru2-O11	179.2(4)
C1–C2	1.371(14)	O10-Ru2-O11	87.7(3)
C1–C14	1.383(13)	O3-Ru2-O12	85.9(3)
C2–C3	1.372(15)	O4-Ru2-O12	176.9(3)
C3–C4	1.417(14)	O9-Ru2-O12	88.2(3)
C4–C5	1.429(14)	O10-Ru2-O12	92.5(3)
C5–C14	1.410(14)	O11-Ru2-O12	91.4(3)
C5–C6	1.451(14)	C13-O1-Ru1	128.9(6)
C6–C7	1.476(14)	C11-O2-Ru1	124.0(6)
C7–C8	1.345(14)	C6-O3-Ru2	128.6(7)
C7–C12	1.428(14)	C4-O4-Ru2	123.4(6)
C8–C9	1.373(17)	C16-O5-Ru1	124.7(8)
C9–C10	1.344(18)	C18-O6-Ru1	124.2(7)
C10–C11	1.433(15)	C21-O7-Ru1	125.1(9)
C11–C12	1.419(15)	C23-O8-Ru1	124.7(9)
C12–C13	1.421(13)	C26-O9-Ru2	122.0(9)
C13–C14	1.441(13)	C28-O10-Ru2	125.5(9)
		C31-O11-Ru2	122.0(7)
		C33-O12-Ru2	121.6(7)
Intraligand bond lengths			
C10–C11	1.433(15)	C3–C4	1.417(14)
C11–C12	1.419(15)	C4–C5	1.429(14)
C12–C13	1.421(13)	C5–C6	1.451(14)
C13–C14	1.441 (13)	C6–C7	1.476(14)
C14–C1	1.383(13)	C7–C8	1.345(14)
C14–C5	1.410(14)	C8–C9	1.373(17)
C1–C2	1.371(14)	C9–C10	1.344(18)
C2–C3	1.372(15)	C7–C12	1.428(14)

1.995 Å) agree well with those of analogous complexes.[20] The average Ru^{III}–O(**L5**$^{2-}$) distance of 1.969 Å is slightly shorter (0.03 Å) than that of Ru–O(acac) bond lengths, indicating a relatively stronger pπ(**L5**$^{2-}$)→dπRu^{III} interaction on either side of the bridging unit. The Ru–Ru distance in **5** is 8.495 Å. It may be noted that, to the best of our knowledge, **5** represents the first structurally characterized dimetal complex of potentially bis-chelating 1,5-dioxido-9,10-anthraquinone; the main result is that the stability of the β-diketonato chelating configuration determines the overall structure and bonding.

The magnetic properties of the compounds will be discussed starting with compound **6**. The magnetic susceptibility of **6** at 10000 G increases from 300 to 2 K (Figure 4a).

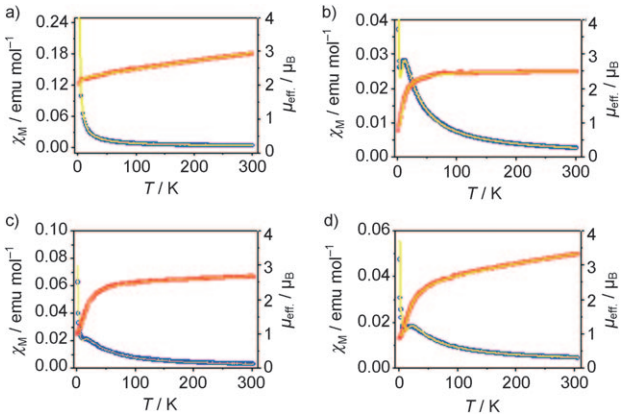

Figure 4. Temperature dependence of the molar susceptibility (blue) and magnetic moment (red) for a) **6**, b) **5**, c) **1**, and d) **2**. Solid lines result from least-squares fits using the model described in the text.

The magnetic moment of 2.92 μ_B at room temperature is slightly higher than that expected for the presence of two isolated unpaired electrons per molecule; however, it drops to 2.02 μ_B at 2 K. The magnetization versus magnetic field measurement from −50000 to 50000 G at 300 K shows a nearly linear variation (Figure S1, Supporting Information). Thus, for magnetic fields higher than 5000 G the magnetization increases linearly with the magnetic field, with lower values than those predicted from Brillouin's function[38] for two paramagnetic $S=^1/_2$ centers ($g=2.00$) and in accordance with the presence of antiferromagnetic interactions. At low-field, the magnetization shows a slight deviation from linearity and reaches values slightly higher than those predicted, suggesting the presence of weak ferromagnetism.[39] The decrease of the magnetic moment on lowering the temperature indicates antiferromagnetic coupling. Although the magnetization versus magnetic field correlation is not strictly linear at room temperature, the magnetic moment and susceptibility have been simulated using Equation (1), which is based on a model that considers the exchange spin Hamiltonian $H=-2JS_1S_2$ operating over two Ru^{III} ($S=^1/_2$) centers that are antiferromagnetically coupled.[40] The presence of a ($S=1$) paramagnetic impurity and temperature-independent paramagnetism (TIP) have also been considered in Equations (1) and (2), respectively.

$$\chi' = (1-P)\chi + P\frac{2Ng^2\beta^2}{3kT} \quad (1)$$

$$\chi = \frac{Ng^2\beta^2}{kT}\frac{2\exp(2J/kT)}{1+3\exp(2J/kT)} + \mathrm{TIP} \quad (2)$$

The terms N, g, β, k, J and T in Equations (1) and (2) have the usual meaning and P is the mole fraction of the noncoupled paramagnetic impurity. The fit of the experimental data using Equation (1) gives good agreement between the experimental and calculated curves (Figure 4a). The parameters obtained in the best fits include a J value of $-0.43\ cm^{-1}$, indicating a very weak antiferromagnetic interaction between the diruthenium(III) centers. The g value of 1.79 is lower than that expected for Ru^{III} compounds, $TIP = 1.59\times10^{-3}\ emu\,mol^{-1}$, $P<10^{-6}\%$. To confirm these parameters, a fit of the magnetic data was also carried out at low temperature (50–2 K) , at which the magnetization versus magnetic field dependence is linear. The alternative parameters, $g=1.76$, $J=-0.31\ cm^{-1}$, $TIP=1.89\times10^{-3}\ emu\,mol^{-1}$, and $P=8.1\times10^{-3}\%$ are similar to those obtained using the full temperature range.

The magnetic moment of structurally characterized **5** at room temperature is 2.45 μ_B, in accordance with two isolated unpaired electrons per molecule. This magnetic moment decreases to 0.77 μ_B at 2 K, indicating a higher degree of antiferromagnetic interaction than that observed for **6** (Figure 4b). The magnetic susceptibility of **5** increases with decreasing temperature and reaches a maximum at 11 K. The magnetization versus magnetic field measurement at 300 K, from −50000 to 50000 G, shows a nearly linear response with values according to the presence of antiferromagnetic interaction. The parameters obtained in the fit using Equation (1) are $TIP=4.19\times10^{-5}\ emu\,mol^{-1}$, $g=2.00$, and $J=-9.00\ cm^{-1}$, indicating a stronger, more moderate magnetic coupling between the ruthenium(III) ions in **5** versus **6**. The J parameter is, however, lower than in [(acac)$_2$Ru(μ-boptz)Ru(acac)$_2$] (boptz = 3,6-bis(2-oxidophenyl)-1,2,4,5-tetrazine; $-36.7\ cm^{-1}$)[41] or [L(acac)Ru(μ-O)Ru(acac)L](PF$_6$)$_2$ (here, L = 1,4,7-trimethyl-1,4,7-triazacyclononane; $-53\ cm^{-1}$).[37l] The fitting procedure implied 10.3% of paramagnetic impurity, suggesting the presence of magnetically nonequivalent species as has been previously reported for diruthenium complexes.[42]

The weaker spin–spin coupling in **6** is confirmed by an intense if poorly resolved EPR signal at $g\approx2.00$ (110 K), while **5** exhibits a very weak EPR response, reflecting enhanced coupling.[43,44] The reason for this difference may lie in the greater dissymmetry in **6**, in which the metals are believed to be bonded more strongly by the peripheral NH donors than by the central O functions.

The complexes **1** and **2** show similar magnetic behavior with magnetic moments of 2.66 and 3.31 μ_B, respectively, at room temperature. The magnetic moment of **1** is close to that expected for two isolated ruthenium centers per molecule, whereas for **2** it is slightly higher. In both complexes, the magnetic moment decreases with decreasing temperature to 1.00 and 0.87 μ_B at 2 K for **1** and **2**, respectively. Thus, the decrease of the magnetic moment with lower temperatures is more pronounced for **2**. In the magnetic susceptibility versus temperature correlations, a shoulder near 20 K and one well-defined maximum at a similar temperature are observed for **1** and **2**, respectively (Figure 4c and d). These maxima indicate antiferromagnetic interactions higher than those calculated for complexes **6** or **5** (Figure 4a and b). On the other hand, the tail at very low temperatures indicates the presence of magnetically nonequivalent species in both complexes.

The magnetization curves at 300 K for **1** and **2** show a similar shape as described for **6**. The magnetization versus magnetic field correlation is not linear and also indicates the presence of weak ferromagnetism at room temperature. Only a tentative fitting of the magnetic data was thus possible yielding values of about $J\approx-13.5\ cm^{-1}$ ($g=2.02$) for **1** and $J\approx-15.5\ cm^{-1}$ ($g=1.99$) for **2**. The most noticeable feature is the stronger antiferromagnetic coupling with respect to the calculated values for **6** and **5**, which indicates better magnetic communication between Ru^{III} in the five-membered chelating ring configuration through the bridging ligands $\mathbf{L1}^{2-}$ and $\mathbf{L2}^{2-}$ in **1** and **2** as compared to Ru^{III} in the six-membered chelating ring configurations offered by the ligands $\mathbf{L5}^{2-}$ and $\mathbf{L6}^{2-}$ in **5** and **6**, respectively.

To evaluate the origin of the ferromagnetism observed at 300 K, several measurements on different samples of complexes **1**, **2**, **5**, and **6** at 300 and 2 K were carried out. In some of these measurements, different magnetization curves for the same compound were obtained. Thus, at 300 K, normal or higher magnetization values were observed, suggesting the presence of a variable ferromagnetic contribution. However, in all cases, the measurements at 2 K show lower values than those predicted by Brillouin's function, indicating the presence of a dominant antiferromagnetic interaction.

The absence of ferromagnetic response at low temperatures suggests that the ferromagnetism in these compounds is probably due to a small quantity of impurity. The ferromagnetic contribution is presumably hidden at low temperature due to the high values of the magnetic susceptibility corresponding to weakly antiferromagnetically coupled complexes. However, the possibility of an intramolecular antiferromagnetic interaction together with intermolecular ferromagnetic exchange enhanced at high temperatures cannot be discarded in these complexes.

Electrochemistry, EPR, and UV/Vis/NIR spectroelectrochemistry: Compounds **1**–**6** display two successive one-electron oxidation steps and three reduction processes (Figure 5, Table 4). The potentials vary depending on the type of L^{2-} associated with the complexes: **2**(X=Cl) > **1**(X=H) > **4**(X=Cl) > **3**(X=H) > **5**(X=O) > **6**(X=NH). The differences in potentials between the successive oxidation (ox1 and ox2, Table 4) and reduction processes (red1, red2, and red3, Table 4) have led to comproportionation constants ($RT\ln K_c = nF(\Delta E)$[45]) in the ranges of $10^{7.8}$–$10^{2.7}$, $10^{14.3}$–$10^{6.1}$, and $10^{15.8}$–$10^{8.3}$, for K_{c1}, K_{c2}, and K_{c3}, respectively (Table 4). In general, the K_c value associated with the oxidation processes appears to be smaller than for the reduction processes. Moreover, K_c changes substantially depending on L^{2-}.

The metal ion (Ru^{III}) as well as the bridging ligand (L^{2-}) in **1**–**6** are in principle susceptible to undergo two-step oxi-

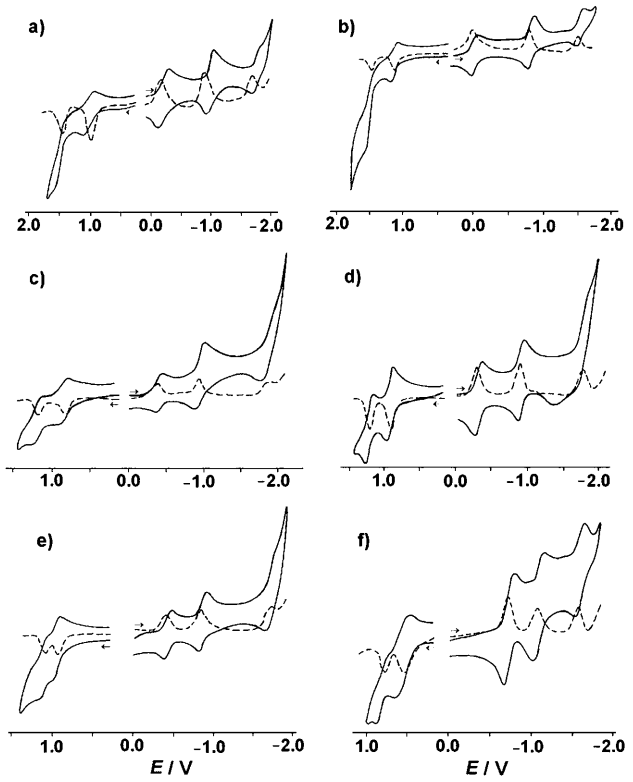

Figure 5. Cyclic voltammograms (——) and differential pulse voltammograms (-----) of a) **1**, b) **2**, c) **3**, d) **4**, e) **5** and f) **6** in CH_3CN/0.1 M NEt_4ClO_4 at 298 K.

dation and reduction processes (Scheme 1); therefore, an attempt has been made to address the question of primary involvement of either the metal- or the ligand-based orbitals towards the observed redox processes (Figure 5, Scheme 1) through EPR and UV/Vis/NIR spectroelectrochemistry in accessible redox states.

In the respective native states, **1**–**6** exhibit EPR spectra (Figure 6) typical for the low-spin Ru^{III} ion.[44] However, the signals are weak and the expected half-field signals at around $g \approx 4$[9a,b], which would correspond to a triplet state, could not be resolved under the experimental conditions, possibly due to complex[8a,41] magnetic exchange processes. The one-electron oxidized ($\mathbf{1}^+$–$\mathbf{6}^+$) or reduced ($\mathbf{1}^-$–$\mathbf{6}^-$) species show similar spectral profiles. Both metal- and ligand-based electron transfer would result in Ru^{III}-centered spin (Schemes 1 and 2). For instance, substance **6** was electrolyzed at the appropriate potential for the amount of time sufficient to produce the oxidized species. A color change from purple to green was observed during electrolysis. There are slight differences in the form of the signals between the nonoxidized **6** and oxidized $\mathbf{6}^+$. Very similar EPR responses for a Ru^{III}/Ru^{III} state and the corresponding Ru^{III}/Ru^{IV} form were observed previously.[8a]

Therefore, the UV/Vis/NIR spectroscopic features of $[\mathbf{1}]^n$–$[\mathbf{6}]^n$ in the accessible redox states (n = +2, +1, 0, −1, and −2) were investigated.

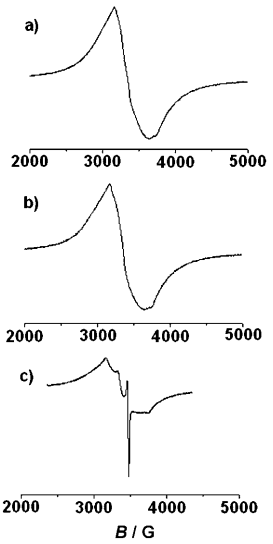

Figure 6. EPR spectra of a) **6**, b) $\mathbf{6}^+$, and c) $\mathbf{6}^-$ in CH_3CN/0.1 M Bu_4NPF_6 at 110 K. The sharp signal at 2.003 in $\mathbf{6}^-$ is attributed to an organic free radical generated during the electrolysis process inside the EPR tube.

Oxidation: Upon one-electron oxidation of **1** or **2** to the corresponding $\mathbf{1}^+$ or $\mathbf{2}^+$ the Ru^{III}-based lowest energy ligand-to-metal charge-transfer (LMCT) band near 600 nm is redshifted to about 700 nm with slight enhancement in intensity. In addition, one moderately intense IVCT band appears in the NIR range at about 1900 nm, which expectedly vanishes on further oxidation to $\mathbf{1}^{2+}$ or $\mathbf{2}^{2+}$ state (Figure 7a,b, Table 5). The appearance of moderately intense NIR IVCT bands in the one-electron oxidized state suggests a preferentially metal-based oxidation leading to a mixed-valent $Ru^{III}Ru^{IV}$ configuration ($[(acac)_2Ru^{III}(\mu\text{-}L^{2-})Ru^{IV}(acac)_2]^+$) instead of the alternative of $[(acac)_2Ru^{III}(\mu\text{-}L^{\bullet-})Ru^{III}(acac)_2]^+$. The band widths at half height ($\Delta\nu_{1/2}$) of the IVCT transitions for $\mathbf{1}^+$ and $\mathbf{2}^+$ were measured as 800 and 980 cm^{-1}, respectively, only slightly lower than the corresponding calculated values of 1091 and 1079 cm^{-1} using the Hush approximation of $\Delta\nu_{1/2} = (2310E_{op})^{1/2}$ for a class II system.[46] This suggests a localized (class II) situation for the mixed-valent $\mathbf{1}^+$ and $\mathbf{2}^+$ although the K_{c1} values of $> 10^6$ (Table 4) could also be compatible with a borderline (class II/III) situation.[4] It may be noted that distinct IVCT bands corresponding to a $Ru^{III}Ru^{IV}$ (d^5/d^4) mixed-valent state have been reported recently for $[(acac)_2Ru^{III}(\mu\text{-}gbha^{2-})Ru^{IV}(acac)_2]^+$ ($gbha^{2-}$ is the dianionic form of glyoxalbis(2-hydroxyanil)),[8a] and in a C_4-linked bis[tris(β-diketonato)ruthenium] complex.[8b] On further oxidation to $\mathbf{1}^{2+}$ or $\mathbf{2}^{2+}$, the LMCT

Table 4. Electrochemical data.[a]

Complex	$E_{1/2}$ (ΔE_{pp})[b]					K_{c1}[c,d]	K_{c2}[c,e]	K_{c3}[c,f]
	ox1	ox2	red1	red2	red3			
1	1.03(90)	1.49(110)	−0.19(70)	−0.90(90)	−1.72(100)	$10^{7.8}$	$10^{12.0}$	$10^{13.9}$
2	1.16(60)	1.51(110)	−0.02(80)	−0.82(90)	−1.51(80)	$10^{5.9}$	$10^{14.3}$	$10^{11.7}$
3	0.84(80)	1.19(70)	−0.39(90)	−0.94(100)	−1.87(120)	$10^{5.9}$	$10^{9.3}$	$10^{15.8}$
4	0.92(90)	1.24(90)	−0.31(80)	−0.89(90)	−1.77(100)	$10^{5.4}$	$10^{9.8}$	$10^{14.9}$
5	0.96(60)	1.12(60)	−0.41(90)	−0.83(90)	−1.71(90)	$10^{2.7}$	$10^{7.1}$	$10^{14.9}$
6	0.58(110)	0.81(100)	−0.71(90)	−1.07(90)	−1.56(100)	$10^{3.9}$	$10^{6.1}$	$10^{8.3}$

[a] From cyclic voltammetry in CH_3CN/0.1 M Et_4NClO_4 at 100 mVs^{-1}. [b] In V versus SCE; peak potential differences ΔE_{pp} [mV] (in parentheses). [c] Comproportionation constant from $RT\ln K_c = nF(\Delta E)$. [d] K_{c1} between ox1 and ox2. [e] K_{c2} between red1 and red2. [f] K_{c3} between red2 and red3.

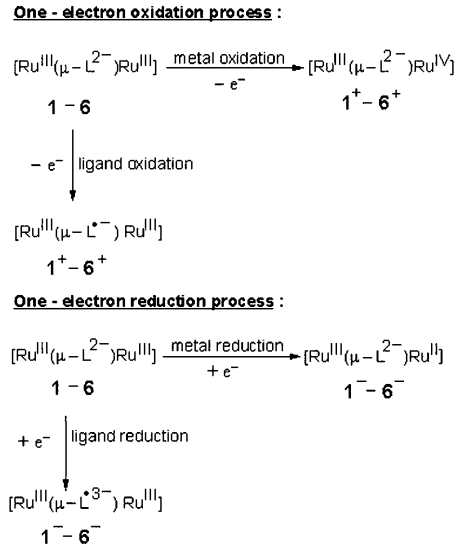

Scheme 2.

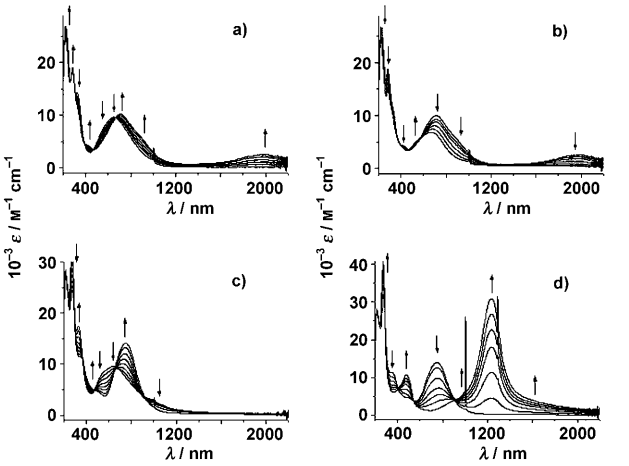

Figure 7. UV/Vis/NIR spectroelectrochemistry for the conversions of a) $\mathbf{2}\rightarrow\mathbf{2}^{+}$, b) $\mathbf{2}^{+}\rightarrow\mathbf{2}^{2+}$, c) $\mathbf{2}\rightarrow\mathbf{2}^{-}$, and d) $\mathbf{2}^{-}\rightarrow\mathbf{2}^{2-}$ in $CH_3CN/0.1\,M$ Bu_4NPF_6.

band is observed to be blue-shifted with substantial decrease in intensity. This is in corroboration with the disappearance of the IVCT band, suggesting either $[(acac)_2Ru^{IV}(\mu\text{-}L^{2-})\,Ru^{IV}(acac)_2]^{2+}$ or $[(acac)_2Ru^{III}(\mu\text{-}L^{0})Ru^{III}(acac)_2]^{2+}$ (more likely) as possible configurations for $\mathbf{1}^{2+}$ or $\mathbf{2}^{2+}$.

Low-energy LMCT bands of **3** and **4** are redshifted from ≈550 to ≈650 nm with appreciable reduction in intensity after oxidation to the $Ru^{III}Ru^{IV}$ state in $\mathbf{3}^{+}$ and $\mathbf{4}^{+}$. These mixed-valent $Ru^{III}Ru^{IV}$ species exhibit intense IVCT bands in the NIR at 1400 nm ($\varepsilon = 5100\,M^{-1}\,cm^{-1}$) and 1430 nm ($\varepsilon = 9800\,M^{-1}\,cm^{-1}$), respectively (Figure 8a, Table 5). The Hush calculated $\Delta\nu_{1/2}$ values of the IVCT bands at 4062 and 4019 cm^{-1}, respectively, are somewhat larger than the experimental values at 3700 and 2590 cm^{-1}, while the K_{c1} values for $\mathbf{3}^{+}$ and $\mathbf{4}^{+}$ are similar at $10^{5.9}$ and $10^{5.4}$. Thus, mixed-valent $\mathbf{3}^{+}$ and $\mathbf{4}^{+}$ are also potential borderline (class II/III) hybrid systems.[4] However, the absence of the typical high-energy cutoff for class II/III species argues against this assignment. On further oxidation to $\mathbf{3}^{2+}$ and $\mathbf{4}^{2+}$, the IVCT transition around 1400 nm vanishes with the concomitant growth of an intense absorption near 1100 nm (Figure 8b). These long-wavelength bands suggest an LMCT transition from the doubly reduced L^{2-} to the oxidized Ru^{IV} centers in $[(acac)_2Ru^{IV}(\mu\text{-}L^{2-})Ru^{IV}$-

Table 5. UV/Vis/NIR spectroelectrochemical data for **1–6**.[a]

Complex	λ_{max} [nm] (ε [$M^{-1}\,cm^{-1}$])
$\mathbf{1}^{2+}$	640(6900), 528(sh), 285(22800)
$\mathbf{1}^{+}$	1940(4000), 1480(sh), 840(sh), 681(12100), 400(sh), 284(24800)
1	605(10700), 344(14800), 284(24600)
$\mathbf{1}^{-}$	980(4600), 776(13700), 485(sh), 425(sh), 352(10400), 273(28700)
$\mathbf{1}^{2-}$	1410(sh), 1184(21700), 980(sh), 502(11400), 475(sh), 271(33700)
$\mathbf{2}^{2+}$	669(6900), 528(sh), 325(sh), 283(14800)
$\mathbf{2}^{+}$	1985(2600), 890(sh), 710(10200), 428(4200), 340(sh), 285(19000)
2	1040(sh), 645(9600), 545(sh), 331(17500), 276(24500)
$\mathbf{2}^{-}$	750(14200), 485(4900), 425(sh), 352(11500), 273(32100)
$\mathbf{2}^{2-}$	1555(sh), 1235(31100), 910(sh), 478(10700), 505(sh), 272(40500)
$\mathbf{3}^{2+}$	1095(7200), 840(sh), 651(9800), 521(9300), 281(26200)
$\mathbf{3}^{+}$	1400(5100), 788(sh), 638(10600), 480(9700), 344(sh), 279(27300)
3	553(16900), 347(12000), 270(27900)
$\mathbf{3}^{-}$	824(23700), 473(sh), 386(13200), 274(34800)
$\mathbf{3}^{2-}$	1180(sh), 917(34500), 807(sh), 489(11900), 355(sh), 272(39600)
$\mathbf{3}^{3-}$	1465(sh), 1136(6400), 899(7100), 654(sh), 578(13000), 520(13700), 427(sh), 347(sh), 271(43500)
$\mathbf{4}^{2+}$	1083(13400), 667(18600), 523(18000), 280(48500)
$\mathbf{4}^{+}$	1430(9800), 802(sh), 646(20100), 492(sh), 345(sh), 279(48300)
4	559(31600), 342(24600), 269(53300)
$\mathbf{4}^{-}$	833(43500), 485(sh), 385(25600), 274(63200)
$\mathbf{4}^{2-}$	1210(sh), 937(71600), 483(23000), 358(16900), 273(74400)
$\mathbf{4}^{3-}$	1555(sh), 1188(16800), 919(17400), 648(sh), 570(27500), 523(29700), 353(sh), 272(78900)
$\mathbf{5}^{2+}$	859(sh), 712(9900), 515(10200), 283(sh)
$\mathbf{5}^{+}$	900(sh), 740(8100), 530(10700), 340(sh), 280(sh), 243(39700)
5	685(6000), 533(13000), 347(11100), 267(28600), 243(34200)
$\mathbf{5}^{-}$	967(19700), 630(sh), 502(8300), 419(12300), 383(12700), 274(33300), 244(37500)
$\mathbf{5}^{2-}$	1255(sh), 970(31600), 481(14500), 437(sh), 360(9000), 274(38300), 240(41600)
$\mathbf{5}^{3-}$	1520(sh), 1200(6900), 870(13200), 788(9600), 710(sh), 603(sh), 567(14200), 503(16100), 360(sh), 267(42800), 248(43600)
$\mathbf{6}^{+}$	702(sh), 617(sh), 554(18700), 488(sh), 447(13500), 330(sh), 267(42100), 234(53600)
6	732(sh), 606(16600), 558(19000), 490(sh), 453(14700), 344(16600), 270(44200), 234(55600)
$\mathbf{6}^{-}$	1205(sh), 961(sh), 867(23700), 578(sh), 441(17900), 389(18700), 272(59400), 236(55700)
$\mathbf{6}^{2-}$	860(32800), 499(sh), 464(18300), 431(sh), 375(15700), 272(62100), 236(59700)
$\mathbf{6}^{3-}$	1101(6500), 862(22300), 785(sh), 640(sh), 545(sh), 489(21900), 377(14600), 271(68500), 236(59400)

[a] In $CH_3CN/0.1\,M$ Bu_4NPF_6.

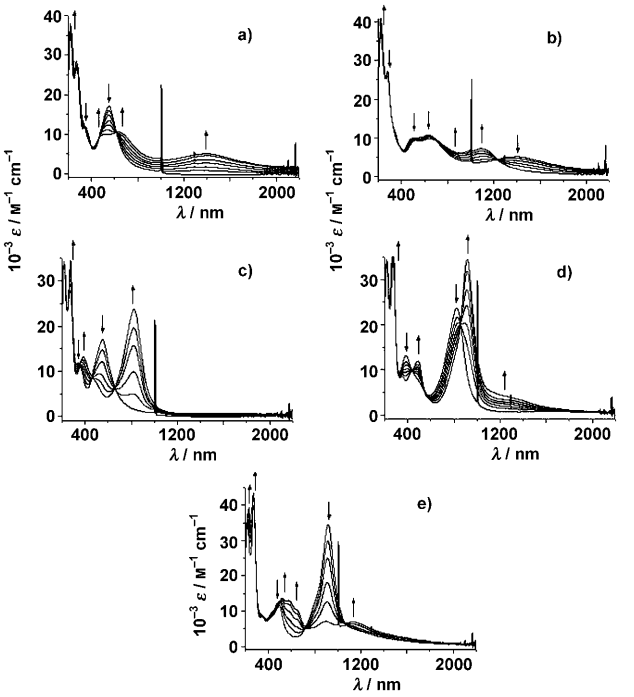

Figure 8. UV/Vis/NIR spectroelectrochemistry for the conversions of a) $\mathbf{3}\rightarrow\mathbf{3}^{+}$, b) $\mathbf{3}^{+}\rightarrow\mathbf{3}^{2+}$, c) $\mathbf{3}\rightarrow\mathbf{3}^{-}$, d) $\mathbf{3}^{-}\rightarrow\mathbf{3}^{2-}$, and e) $\mathbf{3}^{2-}\rightarrow\mathbf{3}^{3-}$ in CH_3CN/0.1 M Bu_4NPF_6.

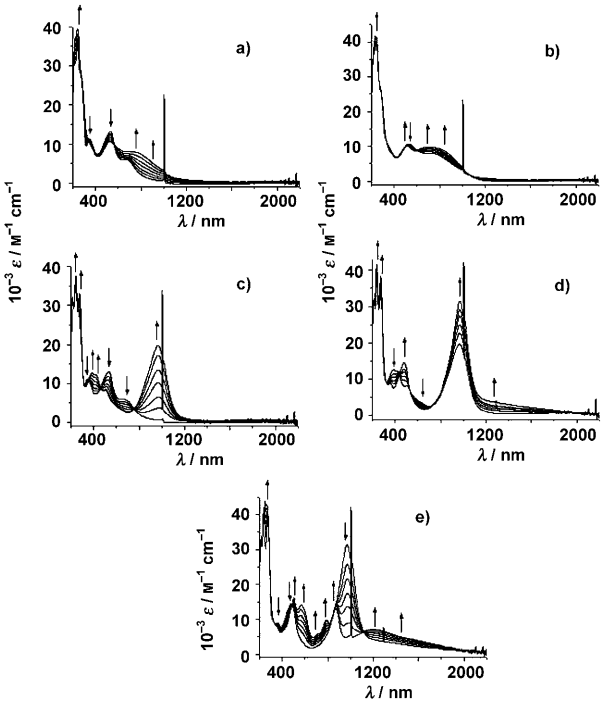

Figure 9. UV/Vis/NIR spectroelectrochemistry for the conversions of a) $\mathbf{5}\rightarrow\mathbf{5}^{+}$, b) $\mathbf{5}^{+}\rightarrow\mathbf{5}^{2+}$, c) $\mathbf{5}\rightarrow\mathbf{5}^{-}$, d) $\mathbf{5}^{-}\rightarrow\mathbf{5}^{2-}$, and e) $\mathbf{5}^{2-}\rightarrow\mathbf{5}^{3-}$ in CH_3CN/0.1 M Bu_4NPF_6.

$(acac)_2]^{2+}$ instead of the alternative formulation $[(acac)_2Ru^{III}(\mu\text{-}L^{0})Ru^{III}(acac)_2]^{2+}$.

On one-electron oxidation of **5** to $\mathbf{5}^{+}$ the lowest energy LMCT transition ($L^{2-}\rightarrow Ru^{III}$) is red-shifted from 685 to 740 nm. However, unlike for $\mathbf{1}^{+}$–$\mathbf{4}^{+}$, a Ru^{III} to Ru^{IV} based IVCT band was not detected in the low-energy NIR region of $\mathbf{5}^{+}$ (Figure 9a). This absence of a low-energy IVCT band in $\mathbf{5}^{+}$ indicates that the first oxidation takes place at the bridging ligand, leading to the formation of a radical-bridged isovalent $[Ru^{III}]_2$ species, $[(acac)_2Ru^{III}(\mu\text{-}L^{\bullet-})Ru^{III}(acac)_2]^{+}$ instead of a mixed-valent alternative such as $[(acac)_2Ru^{III}(\mu\text{-}L^{2-})Ru^{IV}(acac)_2]^{+}$, as was proposed for $\mathbf{1}^{+}$–$\mathbf{4}^{+}$. The doubly oxidized $\mathbf{5}^{2+}$ exhibits a broad LMCT band centered at 712 nm (Figure 9b), suggesting either $[(acac)_2Ru^{III}(\mu\text{-}L^{\bullet-})Ru^{IV}(acac)_2]^{2+}$ or $[(acac)_2Ru^{IV}(\mu\text{-}L^{2-})Ru^{IV}(acac)_2]^{2+}$. The long-wavelength absorption in $\mathbf{5}^{2+}$ is less compatible with the alternative option of a fully oxidized quinone-bridged configuration $[(acac)_2Ru^{III}(\mu\text{-}L^{0})Ru^{III}(acac)_2]^{2+}$. In case of the analogous imine derivative, upon going from **6** to $\mathbf{6}^{+}$, the LMCT band is blue-shifted from 606 to 554 nm, with a slight increase in the intensity; again, no IVCT band is detected in the NIR region (Figure 10a). The doubly oxidized species $\mathbf{6}^{2+}$ was found to be unstable. The absence of a NIR absorption of $\mathbf{6}^{+}$ raises the possibility of the oxidation of the bridging diiminoquinone ligand, leading to the formulation of $[(acac)_2Ru^{III}(\mu\text{-}L^{\bullet-})Ru^{III}(acac)_2]^{+}$ rather than the mixed-valent alternative $[(acac)_2Ru^{III}(\mu\text{-}L^{2-})Ru^{IV}(acac)_2]^{+}$. Thus, metal-based orbitals seem to be primarily involved in the first oxidation processes of the smaller quinone-bridged complexes ($\mathbf{1}^{+}$, $\mathbf{2}^{+}$ and $\mathbf{3}^{+}$, $\mathbf{4}^{+}$),

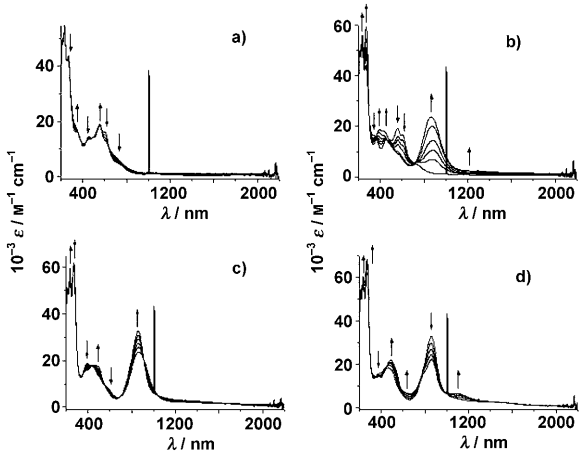

Figure 10. UV/Vis/NIR spectroelectrochemistry for the conversions of a) $\mathbf{6}\rightarrow\mathbf{6}^{+}$, b) $\mathbf{6}\rightarrow\mathbf{6}^{-}$, c) $\mathbf{6}^{-}\rightarrow\mathbf{6}^{2-}$, and d) $\mathbf{6}^{2-}\rightarrow\mathbf{6}^{3-}$ in CH_3CN/0.1 M Bu_4NPF_6.

whereas quinone-based orbitals are the redox-active molecular orbitals (MOs) for the larger quinone-bridged complexes ($\mathbf{5}^{+}$ and $\mathbf{6}^{+}$).

It is remarkable that the spectroelectrochemical response of **5** differs from that of isomeric **7**,[23] reflecting a different π-conjugation pattern and, thus, a different oxidation location based on different orbital ordering. However, systems $\mathbf{3}^{n}$ and $\mathbf{7}^{n}$ display strikingly similar effects such as the broad NIR band emerging after first oxidation (1400 nm for *meso*-$\mathbf{3}^{+}$, 1390 nm for *meso*-$\mathbf{7}^{+}$) and its decrease after second oxidation with concomitant rise of a band at about 1095 nm.

This and the similarly close correspondence on stepwise reduction reflect the similarity of the ligand π structures of $\mathbf{3}^n$ and $\mathbf{7}^n$; which differ only by the annelated benzene ring; in both cases the redox-active MO seems to be metal-centered, whereas the $\mathbf{5}^n$ analogue appears to offer a more ligand-based MO due to more efficient π conjugation.

Reduction: Reduction of **1** or **2** to $\mathbf{1}^-$or $\mathbf{2}^-$ causes LMCT band shifts from about 650 to near 800 nm with appreciable increase in intensity, which is still more pronounced after adding another electron in the doubly reduced species (Table 5). Both $\mathbf{1}^-$ and $\mathbf{2}^-$ failed to show any distinct IVCT bands in the NIR region up to 2000 nm (Figure 7, Table 5). These spectral features are less compatible with a mixed-valent $[(acac)_2Ru^{III}(\mu\text{-}L^{2-})Ru^{II}(acac)_2]^-$ formulation.[41] The alternative interpretation, encompassing the singly reduced form of the bridging ligand in combination with isovalent ruthenium(III) centers, $[(acac)_2Ru^{III}(\mu\text{-}L^{\bullet 3-})Ru^{III}(acac)_2]^-$, appears to be more probable with antiferromagnetic coupling between one Ru^{III} ion and the ligand radical leading to a Ru^{III}-type EPR response. The intense and sharp band near 1200 nm in $\mathbf{1}^{2-}$ or $\mathbf{2}^{2-}$ suggests an LMCT transition of $[(acac)_2Ru^{III}(\mu\text{-}L^{4-})Ru^{III}(acac)_2]^{2-}$ rather than $[(acac)_2Ru^{III}(\mu\text{-}L^{\bullet 3-})Ru^{II}(acac)_2]^{2-}$ or $[(acac)_2Ru^{II}(\mu\text{-}L^{2-})Ru^{II}(acac)_2]^{2-}$.

Similar features of successive red-shifting of the LMCT band ($\approx 550 \rightarrow \approx 800 \rightarrow \approx 900$ nm) along with the enhancement of intensity on moving from **3**/**4**→$\mathbf{3}^-$/$\mathbf{4}^-$→$\mathbf{3}^{2-}$/$\mathbf{4}^{2-}$ and the absence of a NIR band due to an IVCT transition in the $\mathbf{3}^-$/$\mathbf{4}^-$ states (Figure 8, Table 5) signify stepwise ligand-based reductions, $[(acac)_2Ru^{III}(\mu\text{-}L^{2-})Ru^{III}(acac)_2]\rightarrow[(acac)_2Ru^{III}(\mu\text{-}L^{\bullet 3-})Ru^{III}(acac)_2]^-\rightarrow[(acac)_2Ru^{III}(\mu\text{-}L^{4-})Ru^{III}(acac)_2]^{2-}$, respectively. Further reduction to $\mathbf{3}^{3-}$ or $\mathbf{4}^{3-}$ leads to a substantial decrease in the intensity of the band near 900 nm, with the simultaneous growth of a new metal-to-ligand charge transfer (MLCT) band near 550 nm. Moreover, an intense low-energy (NIR, Table 5, Figure 8) absorption band near 1100 nm has been observed for $\mathbf{3}^{3-}$/$\mathbf{4}^{3-}$, suggesting a delocalized $[(acac)_2Ru^{III}(\mu\text{-}L^{4-})Ru^{II}(acac)_2]^{3-}$ configuration.[4d]

The spectral features of the successive reduced states of the larger anthraquinone-derived $\mathbf{5}^-$/$\mathbf{6}^-$, $\mathbf{5}^{2-}$/$\mathbf{6}^{2-}$, and $\mathbf{5}^{3-}$/$\mathbf{6}^{3-}$ are very similar to those of the benzoquinone and napthoquinone complexes, leading to the formulations of $[(acac)_2Ru^{III}(\mu\text{-}L^{\bullet 3-})Ru^{III}(acac)_2]^-\rightarrow[(acac)_2Ru^{III}(\mu\text{-}L^{4-})Ru^{III}(acac)_2]^{2-}\rightarrow[(acac)_2Ru^{III}(\mu\text{-}L^{4-})Ru^{II}(acac)_2]^{3-}$, respectively.

Conclusion

By using three different kinds of *p*-quinones with deprotonated OH or NH_2 substituents in suitable positions for double metal chelation we have shown that the reaction with $[Ru(acac)_2(CH_3CN)_2]$ yields bridged dinuclear complexes with antiferromagnetically coupled ruthenium(III) centers. The magnetic coupling, although complicated by ferromagnetic contributions, shows higher *J* values for the smaller systems. Similarly, the electrochemical comproportionation constants K_c for two reversible oxidative and two reversible reductive one-electron processes were found to be larger for the smaller π systems **1** and **2** as compared to naphthoquinone (**3**/**4**) and anthraquinone (**5**/**6**) complexes. Chloride substitution (**1**/**2** and **3**/**4**) and the O^-/NH^- exchange (**5**/**6**) gave the expected effects from decreasing and increasing the electron density, respectively. Comparison of the previously studied **7** with the isomeric **5** showed not only qualitative but also quantitative differences, which could be rationalized based on the similarity of electronic structures and spectral features of **3** and **7**. While EPR was inconclusive, the UV/Vis/NIR spectroelectrochemistry supported reduction and oxidation of the ligand for the larger π systems **5** and **6** (Scheme 3). With the smaller bridging ligands and their larger HOMO–LUMO gaps in **1**–**4,** the oxidation to $\mathbf{1}^+$–$\mathbf{4}^+$ produces near infrared absorptions, which we have assigned to IVCT transitions of $Ru^{III}Ru^{IV}$ mixed-valent species. Analysis according to Hush suggests localized (class II) to class II/III borderline descriptions of the valence situation. Reduction to $\mathbf{1}^-$–$\mathbf{4}^-$ occurs predominantly on the ligand (Scheme 3).

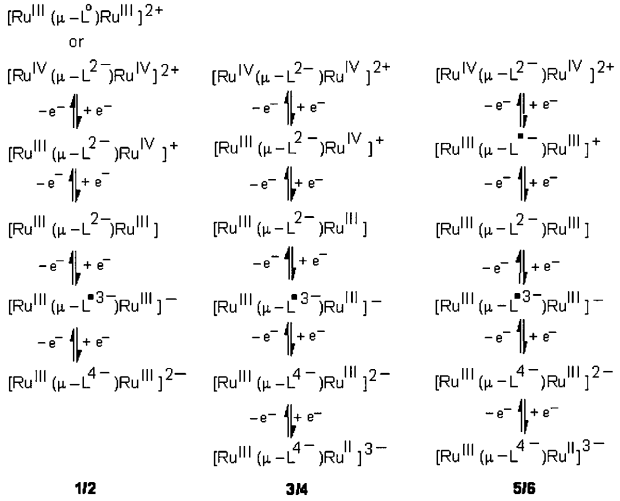

Scheme 3.

Experimental Section

Materials and instrumentations: The starting complex $[Ru(acac)_2(CH_3CN)_2]$ was prepared according to the reported procedure.[47] The ligands 2,5-dihydroxy-1,4-benzoquinone (H_2**L1**), 2,5-dihydroxy-3,6-dichloro-1,4-benzoquinone (H_2**L2**), 5,8-dihydroxy-1,4-naphthoquinone

(H_2**L3**), 2,3-dichloro-5,8-dihydroxy-1,4-naphthoquinone (H_2**L4**), 1,5- dihydroxy-9,10-anthraquinone (H_2**L5**) and 1,5-diamino-9,10-anthraquinone (H_2**L6**) were purchased from Aldrich (USA). Other chemicals and solvents were reagent grade and used as received. For spectroscopic and electrochemical studies HPLC grade solvents were used.

UV/Vis/NIR spectroelectrochemical studies were performed in CH_3CN/0.1 M Bu_4NPF_6 at 298 K using an optically transparent thin-layer electrode (OTTLE) cell[48] mounted in the sample compartment of a J&M Tidas spectrophotometer. FTIR spectra were taken on a Nicolet spectrophotometer with samples prepared as KBr pellets. Solution electrical conductivity was checked by using a Systronic 305 conductivity bridge. ^{1}H NMR spectra were obtained with a 400 MHz Varian FT spectrometer. The EPR measurements were performed in a two-electrode capillary tube[49] with an X-band Bruker system ESP300, equipped with a Bruker ER035 M gaussmeter and a HP 5350B microwave counter. Cyclic voltammetric, differential pulse voltammetric, and coulometric measurements were carried out using a PAR model 273 A electrochemistry system. Platinum wire working and auxiliary electrodes and an aqueous saturated calomel reference electrode (SCE) were used in a three-electrode configuration. The supporting electrolyte was Et_4NClO_4 and the solute concentration was approximately 10^{-3} M. The half-wave potential E^o_{298} was set equal to $0.5(E_{pa}+E_{pc})$, in which E_{pa} and E_{pc} are anodic and cathodic cyclic voltammetric peak potentials, respectively. A platinum-wire gauze working electrode was used in coulometric experiments. All experiments were carried out under a nitrogen atmosphere. The elemental analysis was carried out with a Perkin–Elmer 240C elemental analyzer. Electrospray mass spectra were recorded on a Micromass Q-ToF mass spectrometer.

[{(acac)$_2$Ru^{III}}$_2$(μ-L1^{2-})] (1) and [{(acac)$_2$Ru^{III}}$_2$(μ-L2^{2-})] (2): The ligands H_2**L1** (0.018 g, 0.13 mmol) and H_2**L2** (0.027 g, 0.13 mmol) were each separately added to a solution of $[Ru(acac)_2(CH_3CN)_2]$ (0.10 g, 0.26 mmol) in of ethanol (20 mL) in the presence of excess NEt_3 (0.09 mL, 0.65 mmol) as a base and the mixtures were heated to reflux for 12 h under atmospheric conditions. The initial orange solutions gradually changed to blue. The reaction mixtures were evaporated to dryness under reduced pressure. The solid masses thus obtained were then purified using a silica gel column. Initially, a red compound corresponding to $[Ru(acac)_3]$ was eluted by CH_2Cl_2/CH_3CN (25:1 v/v), followed by a blue compound with CH_2Cl_2/CH_3CN (15:1 v/v) in each case, corresponding to **1** and **2**. Evaporation of the solvents under reduced pressure yielded pure complexes **1** and **2**.

Data for ***1***: Yield: 0.025 g (26%); elemental analysis calcd (%) for $C_{26}H_{30}O_{12}Ru_2$: C 42.28, H 4.10; found: C 42.60, H, 4.15; ^{1}H NMR (400 MHz, $CDCl_3$, 298 K): $\delta = -22.34$ (3H), −21.84 (3H), −19.19 (3H), −18.80 (3H; 4CH_3(acac)), −10.12 (1H), −9.60 (1H; 2CH(acac)), 5.29 ppm (2H; 2CH(**L1**$^{2-}$)).

Data for ***2***: Yield: 0.03 g (28%); elemental analysis calcd (%) for $C_{26}H_{28}O_{12}Cl_2Ru_2$: C 38.71, H 3.50; found: C 38.39, H, 3.59; ^{1}H NMR (400 MHz, $CDCl_3$, 298 K): $\delta = -23.92$ (3H), −23.53 (3H), −21.14 (3H), −20.68 (3H; 4CH_3(acac)), −14.19 (1H), −13.68 ppm (1H;2CH(acac)).

[{(acac)$_2$Ru^{III}}$_2$(μ-L3^{2-})] (3) and [{(acac)$_2$Ru^{III}}$_2$(μ-L4^{2-})] (4): The ligands H_2**L3** (0.024 g, 0.13 mmol) and H_2**L4** (0.033 g, 0.13 mmol) were each separately dissolved in a solution of $[Ru(acac)_2(CH_3CN)_2]$ (0.10 g, 0.26 mmol) in ethanol (20 mL) in the presence of excess NEt_3 (0.09 mL, 0.65 mmol) as a base and the mixtures were heated to reflux for 12 h under atmospheric conditions. The initial orange solutions gradually changed to violet. The reaction mixtures were evaporated to dryness under reduced pressure. The resultant solid masses were purified using silica gel column. Initially, a red solution of $[Ru(acac)_3]$ was eluted by CH_2Cl_2/CH_3CN (25:1 v/v), followed by a violet compound in each case with CH_2Cl_2/CH_3CN (4:1 v/v), corresponding to **3** and **4**. Evaporation of the solvents under reduced pressure yielded pure complexes **3** and **4**.

Data for ***3***: Yield: 0.035 g (34%); elemental analysis calcd (%) for $C_{30}H_{32}O_{12}Ru_2$: C 45.69, H 4.09; found: C 45.31, H, 4.17.

Data for ***4***: Yield: 0.03 g (27%); elemental analysis calcd (%) for $C_{30}H_{30}O_{12}Cl_2Ru_2$: C 42.06, H 3.53; found: C 42.24, H, 3.64.

[{(acac)$_2$Ru^{III}}$_2$(μ-L5^{2-})] (5) and [{(acac)$_2$Ru^{III}}$_2$(μ-L6^{2-})] (6): The ligands H_2**L5** (0.031 g, 0.13 mmol) and H_2**L6** (0.031 g, 0.13 mmol) were each separately mixed in a solution of $[Ru(acac)_2(CH_3CN)_2]$ (0.10 g, 0.26 mmol) in ethanol (20 mL) and excess NEt_3 (0.09 mL, 0.65 mmol) was added as a base. The mixture was then heated to reflux for 12 h under atmospheric conditions. The initial orange solutions gradually changed to reddish-purple. The reaction mixtures were evaporated to dryness under reduced pressure. The solid masses thus obtained were then purified using a silica gel column. Initially, a red compound corresponding to $[Ru(acac)_3]$ was eluted by CH_2Cl_2/CH_3CN (4:1 v/v), followed by purple-red and purple compounds with CH_2Cl_2/CH_3CN (3:2 v/v) corresponding to **5** and **6**, respectively. Evaporation of solvent under reduced pressure yielded pure complexes **5** and **6**.

Data for ***5***: Yield: 0.04 g (36%); elemental analysis calcd (%) for $C_{34}H_{34}O_{12}Ru_2$: C 48.69, H 4.09; found: C 48.76, H, 4.07; ^{1}H NMR (400 MHz, $CDCl_3$, 298 K): $\delta = -17.98$ (3H), −16.65 (3H), −15.49 (3H), −13.62 (3H), −2.40 (3H), −1.04 (3H), 2.83 (3H), 1.68 (3H; 8CH_3-(acac)), −8.49 (1H), −8.33 (1H), −5.93 (1H), −5.55 (1H; 4CH(acac)) −20.40 (1H), −7.02 (1H), 4.32 (2H), 18.25 (1H), 18.56 ppm (1H; 6CH-(**L5**$^{2-}$)).

Data for ***6***: Yield: 0.025 g (23%); elemental analysis calcd (%) for $C_{34}H_{36}O_{10}N_2Ru_2$: C 48.80, H 4.34; found: C 48.68, H, 4.36; ^{1}H NMR (400 MHz, $CDCl_3$, 298 K): $\delta = 7.26$ (3H), 5.30 (3H), 1.58 (6H; 4CH_3-(acac)) −25.12 (1H), −45.19 (1H; 2CH(acac)), 3.02 (1H), −0.28 (1H), −4.39 ppm (1H; 3CH(**L6**$^{2-}$)).

Magnetic susceptibility measurements: The variable-temperature magnetic susceptibilities were measured on polycrystalline samples with a Quantum Design MPMSXL SQUID (Superconducting Quantum Interference Device) susceptometer over a temperature range of 2 to 300 K at a constant field of 10000 G. Each raw data field was corrected for the diamagnetic contribution of both the sample holder and the complex to the susceptibility. The molar diamagnetic corrections were calculated on the basis of Pascal constants. The fit of the experimental data was carried out using the MATLAB V.5.1.0.421 program. Magnetization measurements were carried out at 2 and 300 K in the −50000 to +50000 G range.

Crystallography: Single crystals were grown by slow evaporation of a 1:1 CH_2Cl_2/CH_3OH mixture of **5**. The crystal data of **5**·0.25H_2O were collected on a Bruker SMART APEX CCD diffractometer at 293 K. Selected data collection parameters and other crystallographic results are summarized in Table 2. All data were corrected for Lorentz polarization and absorption effects. The program package of SHELX-97 (SHELXTL)[50,51] was used for structure solution and full-matrix least-squares refinement on F^2. Hydrogen atoms were included in the refinement using the riding model. Contributions of H atoms for the water molecules were included but were not fixed. CCDC-685676 contains the supplementary crystallographic data for this paper. These data can be obtained free of charge from The Cambridge Crystallographic Data Centre via www.ccdc.cam.ac.uk/data_request/cif.

Acknowledgements

Financial support received from the Department of Science and Technology and Council of Scientific and Industrial Research, New Delhi (India); the DAAD, the DFG, and the Fonds der Chemischen Industrie (Germany); the Spanish M.E.C. (CTQ 2005—00397); and C.A.M. (S-0505-MAT-0303), is gratefully acknowledged.

[1] a) W. Kaim, G. K. Lahiri, *Angew. Chem.* **2007**, *119*, 1808; *Angew. Chem. Int. Ed.* **2007**, *46*, 1778; b) V. Balzani, M. Venturi, A. Credi, *Molecular Devices and Machines: A Journey into the Nanoworld*, Wiley-VCH, Weinheim, Germany, **2003**; c) *Molecular Switches* (Ed.: B. L. Feringa), Wiley-VCH, Weinheim (Germany), **2001**; d) F. Paul, C. Lapinte, *Coord. Chem. Rev.* **1998**, *178–180*, 431; e) M. D. Ward, *Chem. Ind.* **1997**, 640; f) M. D. Ward, *Chem. Ind.* **1996**, 568; g) O. Kahn, J.-P. Launay, *Chemtronics* **1988**, *3*, 140; h) S. Fraysse, C. Coudret, J.-P. Launay, *J. Am. Chem. Soc.* **2003**, *125*, 5880; i) S. Fraysse, C. Coudret, J.-P. Launay, *Eur. J. Inorg. Chem.* **2000**, 1581; j) M. D.

Ward, *J. Chem. Educ.* **2001**, *78*, 321; k) L. F. Joulié, E. Schatz, M. D. Ward, F. Weber, L. J. Yellowlees, *J. Chem. Soc. Dalton Trans.* **1994**, 799; l) J.-P. Launay, *Chem. Soc. Rev.* **2001**, *30*, 386; m) V. C. Lau, L. A. Berben, J. R. Long, *J. Am. Chem. Soc.* **2002**, *124*, 9042; n) S. B. Braun-Sand, O. Wiest, *J. Phys. Chem. B* **2003**, *107*, 9624; o) S. B. Braun-Sand, O. Wiest, *J. Phys. Chem. A* **2003**, *107*, 285; p) C. S. Lent, B. Iskasen, M. Lieberman, *J. Am. Chem. Soc.* **2003**, *125*, 1056.

[2] a) E. I. Solomon, T. C. Brunold, M. I. Davis, J. N. Kemsley, S. K. Lee, N. Lehnert, F. Neese, A. J. Skulan, Y. S. Yang, J. Zhou, *Chem. Rev.* **2000**, *100*, 235; b) E. I. Solomon, X. Xie, A. Dey, *Chem. Soc. Rev.* **2008**, *37*, 623.

[3] a) W. Kaim, B. Sarkar, *Coord. Chem. Rev.* **2007**, *251*, 584; b) D. M. D'Alessandro, F. R. Keene, *Chem. Soc. Rev.* **2006**, *35*, 424; c) D. M. D'Alessandro, F. R. Keene, *Chem. Rev.* **2006**, *106*, 2270; d) D. M. D'Alessandro, F. R. Keene, *Chem. Eur. J.* **2005**, *11*, 3679; e) R. J. Crutchley, *Angew. Chem.* **2005**, *117*, 6610; *Angew. Chem. Int. Ed.* **2005**, *44*, 6452; f) B. S. Brunschwig, N. Sutin, *Coord. Chem. Rev.* **1999**, *187*, 233; g) D. E. Richardson, H. Taube, *Coord. Chem. Rev.* **1984**, *60*, 107; h) R. J. Crutchley, *Comprehensive Coordination Chemistry II* (Eds.: J. A. McCleverty, T. J. Meyer), Elsevier, Amsterdam, **2004**, p. 235; i) J. T. Hupp, *Comprehensive Coordination Chemistry II* (Eds.: J. A. McCleverty, T. J. Meyer), Elsevier, Amsterdam, **2004**, p. 709; j) B. K. Breedlove, T. Yamaguchi, T. Ito, C. H. Londergan, C. P. Kubiak, *Comprehensive Coordination Chemistry II* (Eds.: J. A. McCleverty, T. J. Meyer), Elsevier, Amsterdam, **2004**, p. 717; k) J. A. McCleverty, M. D. Ward, *Acc. Chem. Res.* **1998**, *31*, 842; l) D. Astruc, *Acc. Chem. Res.* **1997**, *30*, 383; m) M. D. Ward, *Chem. Soc. Rev.* **1995**, *24*, 121; n) G. Giuffrida, S. Campagna, *Coord. Chem. Rev.* **1994**, *135–136*, 517; o) R. J. Crutchley, *Adv. Inorg. Chem.* **1994**, *41*, 273; p) W. Kaim, A. Klein, M. Glöckle, *Acc. Chem. Res.* **2000**, *33*, 755; q) W. Kaim, *Coord. Chem. Rev.* **2002**, *230*, 126; r) B. S. Brunschwig, C. Creutz, N. Sutin, *Chem. Soc. Rev.* **2002**, *31*, 168; s) N. Shan, S. J. Vickers, H. Adams, M. D. Ward, J. A. Thomas, *Angew. Chem.* **2004**, *116*, 4028; *Angew. Chem. Int. Ed.* **2004**, *43*, 3938; t) S. Kar, N. Chanda, S. M. Mobin, A. Datta, F. A. Urbanos, V. G. Puranik, R. Jimenez -Aparicio, G. K. Lahiri, *Inorg. Chem.* **2004**, 43, 4911; u) B. Sarkar, W. Kaim, A. Klein, B. Schwederski, J. Fiedler, C. Duboc-Toia, G. K. Lahiri, *Inorg. Chem.* **2003**, *42*, 6172; v) S. Patra, T. A. Miller, B. Sarkar, M. Niemeyer, M. D. Ward, G. K. Lahiri, *Inorg. Chem.* **2003**, *42*, 4707; w) S. Kar, T. A. Miller, S. Chakraborty, B. Sarkar, B. Pradhan, R. K. Sinha, T. Kundu, M. D. Ward, G. K. Lahiri, *Dalton Trans.* **2003**, 2591; x) S. Patra, B. Mondal, B. Sarkar, M. Niemeyer, G. K. Lahiri, *Inorg. Chem.* **2003**, *42*, 1322; y) S. Chakraborty, R. H. Laye, P. Munshi, R. L. Paul, M. D. Ward, G. K. Lahiri, *J. Chem. Soc. Dalton Trans.* **2002**, 2348; z) B. Sarkar, R. H. Laye, B. Mondal, S. Chakraborty, R. L. Paul, J. C. Jeffery, V. G. Puranik, M. D. Ward, G. K. Lahiri, *J. Chem. Soc. Dalton Trans.* **2002**, 2097.

[4] a) M. Koley, B. Sarkar, S. Ghumaan, E. Bulak, J. Fiedler, W. Kaim, G. K. Lahiri, *Inorg. Chem.* **2007**, *46*, 3736; b) S. Ghumaan, B. Sarkar, N. Chanda, M. Sieger, J. Fiedler, W. Kaim, G. K. Lahiri, *Inorg. Chem.* **2006**, *45*, 7955; c) N. Chanda, B. Sarkar, S. Kar, J. Fiedler, W. Kaim, G. K. Lahiri, *Inorg. Chem.* **2004**, *43*, 5128; d) N. Chanda, B. Sarkar, J. Fiedler, W. Kaim, G. K. Lahiri, *Dalton Trans.* **2003**, 3550; e) N. Chanda, R. H. Laye, S. Chakraborty, R. L. Paul, J. C. Jeffery, M. D. Ward, G. K. Lahiri, *J. Chem. Soc. Dalton Trans.* **2002**, 3496; f) K. D. Demadis, C. M. Hartshorn, T. J. Meyer, *Chem. Rev.* **2001**, *101*, 2655; g) R. C. Rocha, F. N. Rein, H. Jude, A. P. Shreve, J. J. Concepcion, T. J. Meyer, *Angew. Chem.* **2008**, *120*, 513; *Angew. Chem. Int. Ed.* **2008**, *47*, 503.

[5] M. B. Robin, P. Day, *Adv. Inorg. Chem. Radiochem.* **1968**, *10*, 247.

[6] a) S. Patra, B. Sarkar, S. Ghumaan, J. Fiedler, W. Kaim, G. K. Lahiri, *Inorg. Chem.* **2004**, *43*, 6108; b) S. Patra, B. Sarkar, S. Ghumaan, J. Fiedler, W. Kaim, G. K. Lahiri, *Dalton Trans.* **2004**, 754; c) S. Chellamma, M. Lieberman, *Inorg. Chem.* **2001**, *40*, 3177.

[7] a) B. Sarkar, S. Patra, J. Fiedler, R. B. Sunoj, D. Janardanan, S. M. Mobin, M. Niemeyer, G. K. Lahiri, W. Kaim, *Angew. Chem.* **2005**, *117*, 5800; *Angew. Chem. Int. Ed.* **2005**, *44*, 5655; b) B. Sarkar, S. Patra, J. Fiedler, R. B. Sunoj, D. Janardanan, G. K. Lahiri, W. Kaim, *J. Am. Chem. Soc.* **2008**, *130*, 3532.

[8] a) S. Kar, B. Sarkar, S. Ghumaan, D. Roy, F. A. Urbanos, J. Fiedler, R. B. Sunoj, R. Jimenez-Aparicio, W. Kaim, G. K. Lahiri, *Inorg. Chem.* **2005**, *44*, 8715; b) Y. Hoshino, S. Higuchi, J. Fiedler, C.-Y. Su, A. Knödler, B. Schwederski, B. Sarkar, H. Hartmann, W. Kaim, *Angew. Chem.* **2003**, *115*, 698; *Angew. Chem. Int. Ed.* **2003**, *42*, 674.

[9] a) S. Kar, B. Sarkar, S. Ghumaan, D. Janardanan, van J. Slageren, J. Fiedler, V. G. Puranik, R. B. Sunoj, W. Kaim, G. K. Lahiri, *Chem. Eur. J.* **2005**, *11*, 4901; b) S. Ghumaan, B. Sarkar, S. Patra, van J. Slageren, J. Fiedler, W. Kaim, G. K. Lahiri, *Inorg. Chem.* **2005**, *44*, 3210; c) S. Patra, B. Sarkar, S. Ghumaan, J. Fiedler, S. Zalis, W. Kaim, G. K. Lahiri, *Dalton Trans.* **2004**, 750; d) S. Chakraborty, R. H. Laye, R. L. Paul, R. G. Gonnade, V. G. Puranik, M. D. Ward, G. K. Lahiri, *J. Chem. Soc. Dalton Trans.* **2002**, 1172; e) S. Frantz, J. Rall, I. Hartenbach, T. Schleid, S. Zalis, W. Kaim, *Chem. Eur. J.* **2004**, *10*, 149; f) J. Rall, A. F. Stange, K. Hubler, W. Kaim, *Angew. Chem.* **1998**, *110*, 2827; *Angew. Chem. Int. Ed.* **1998**, *37*, 2681.

[10] a) S. Patra, B. Sarkar, S. M. Mobin, W. Kaim, G. K. Lahiri, *Inorg. Chem.* **2003**, *42*, 6469; b) C. Remenyi, M. Kaupp, *J. Am. Chem. Soc.* **2005**, *127*, 11399; c) S. Maji, S. Patra, S. Chakraborty, S. M. Mobin, D. Janardanan, R. B. Sunoj, G. K. Lahiri, *Eur. J. Inorg. Chem.* **2007**, 314; d) M. Elhabiri, O. Siri, A. Sornosa-Tent, A.-M. Albrecht-Gary, P. Braunstein, *Chem. Eur. J.* **2004**, *10*, 134; e) P. Braunstein, A. Demessence, O. Siri, J.-P. Taquet, *C. R. Chimie* **2004**, *7*, 909; f) O. Siri, P. Braunstein, M. M. Rohmer, M. Bénard, R. Welter, *J. Am. Chem. Soc.* **2003**, *125*, 13793; g) O. Siri, P. Braunstein, *Chem. Commun.* **2000**, 2223; h) H. Adams, X. Chen, B. E. Mann, *J. Chem. Soc. Dalton Trans.* **1996**, 2159; i) A. Elduque, Y. Garces, L. A. Oro, M. T. Pinillos, A. Tiripicchio, F. Ugozzoli, *J. Chem. Soc. Dalton Trans.* **1996**, 2155; j) C. Fujii, M. Mitsumi, M. Kodera, K.-I. Motoda, M. Ohba, N. Matsumoto, H. Okawa, *Polyhedron* **1994**, *13*, 933; k) M. A. Calvo, A. M. M. Lanfredi, L. A. Oro, M. T. Pinillos, C. Tejel, A. Tiripicchio, F. Ugozzoli, *Inorg. Chem.* **1993**, *32*, 1147; l) K. Lu, J. E. Earley, *Inorg. Chem.* **1993**, *32*, 189; m) S. Liu, S. N. Shaikh, J. Zubieta, *J. Chem. Soc. Chem. Commum.* **1988**, 1017; n) C. G. Pierpont, L. C. Francesconi, D. N. Hendrickson, *Inorg. Chem.* **1977**, *16*, 2367; o) C. G. Pierpont, H. H. Downs, *J. Am. Chem. Soc.* **1975**, *97*, 2123; p) S. I. Gorelsky, A. B. P. Lever, M. Ebadi, *Coord. Chem. Rev.* **2002**, *230*, 97; q) C. G. Pierpont, C. W. Lange, *Prog. Inorg. Chem.* **1994**, *41*, 331; r) P. Chaudhuri, C. N. Verani, E. Bill, E. Bothe, T. Weyhermüller, K. Wieghardt, *J. Am. Chem. Soc.* **2001**, *123*, 2213; s) P. Ghosh, A. Begum, D. Herebian, E. Bothe, K. Hildenbrand, T. Weyhermüller, K. Wieghardt, *Angew. Chem.* **2003**, *115*, 581; *Angew. Chem. Int. Ed.* **2003**, *42*, 563; t) A. DelMedico, E. S. Dodsworth, A. B. P. Lever, W. J. Pietro, *Inorg. Chem.* **2004**, *43*, 2654; u) C. J. da Cunha, E. S. Dodsworth, M. A. Monteiro, A. B. P. Lever, *Inorg. Chem.* **1999**, *38*, 5399.

[11] a) *Biochemistry of Quinones* (Ed.: R. A. Morton), Academic Press, New York, **1965**; b) B. Furie, B. A. Bouchard, B. C. Furie, *Blood* **1999**, *93*, 1798.

[12] Y. Izumi, H. Sawada, N. Sakka, N. Yamamoto, T. Kume, H. Katsuki, S. Shimohama, A. Akaike, *J. Neurosci. Res.* **2005**, *79*, 849.

[13] C. A. Wraight, *Front. Biosci.* **2004**, *9*, 309.

[14] a) C. Anthony, *Biochem. J.* **1996**, *320*, 697; b) C. Anthony, *Arch. Biochem. Biophys.* **2004**, *428*, 2.

[15] J. Koyama, *Recent Pat. Anti-Infect. Drug Discovery* **2006**, *1*, 113.

[16] a) M. He, P. J. Sheldon, D. H. Sherman, *Proc. Natl. Acad. Sci. USA* **2001**, *98*, 926; b) G. G. Sadler, N. R. Gordon, *Inorg. Chim. Acta* **1991**, *180*, 271; c) J. Butler, B. M. Hoey, *Br. J. Cancer Suppl.* **1987**, *55*, 53.

[17] W. Sun, K. Jiao, *Talanta* **2002**, *56*, 1073.

[18] a) W. Sun, T. H. Patton, L. K. Stultz, J. P. Claude, *Opt. Commun.* **2003**, *218*, 189; b) T. Mukherjee, *Proc. Indian Natl. Sci. Acad. A* **2000**, *66 A*, 239.

[19] a) "Anthraquinone Dyes and Intermediates": H.-S. Bien, J. Stawitz, K. Wunderlich in *Ullmann's Encyclopedia of Industrial Chemistry Vol. 3*, Wiley-VCH, Weinheim, **2005**, 1; b) A. B. dos Santos, I. A. E.

Bisschops, F. J. Cervantes, J. B. van Lier, *J. Biotechnol.* **2005**, *115*, 345.
[20] G. Goor, J. Glenneberg, S. Jacobi, "*Hydrogen Peroxide*" in *Ullmann's Encyclopedia of Industrial Chemistry*, Wiley, Weinheim, **2007**, 1.
[21] a) S. Ernst, P. Hänel, J. Jordanov, W. Kaim, V. Kasack, E. Roth, *J. Am. Chem. Soc.* **1989**, *111*, 1733; b) C. Mukherjee, T. Weyhermüller, E. Bothe, P. Chaudhuri, *Inorg. Chem.* **2008**, *47*, 2740; c) T. Kretz, J. W. Bats, S. Losi, B. Wolf, H.-W. Lerner, M. Lang, P. Zanello, M. Wagner, *Dalton Trans.* **2006**, 4914.
[22] a) M. Haga, A. B. P. Lever, *Inorg. Chem.* **1986**, *25*, 447; b) C. G. Pierpont, *Coord. Chem. Rev.* **2001**, *219–221*, 415; c) W. P. Griffith, *Transition Met. Chem.* **1993**, *18*, 250.
[23] S. Maji, B. Sarkar, S. M. Mobin, J. Fiedler, F. A. Urbanos, R. Jimenez-Aparicio, W. Kaim, G. K. Lahiri, *Inorg. Chem.* **2008**, *47*, 5204.
[24] A. K. Gupta, R. K. Poddar, A. Choudhury, *Indian J. Chem. A* **2000**, *39*, 1191.
[25] M. D. Ward, *Inorg. Chem.* **1996**, *35*, 1712.
[26] S. I. Mostafa, S. P. Perlepes, N. Hadjiliadis, *Z. Naturforsch. B* **2001**, *56*, 394.
[27] A. K. Gupta, A. Gupta, A. Choudhury, *Indian J. Chem. A* **2002**, *41*, 2076.
[28] I. Ando, N. Saeki, T. Hamaghi, K. Ujimoto, H. Kurihara, *Fukuoka Daigaku Rigaku Shuho* **2002**, *32*, 13.
[29] S. Ghumaan, S. Mukherjee, S. Kar, D. Roy, S. M. Mobin, R. B. Sunoj, G. K. Lahiri, *Eur. J. Inorg. Chem.* **2006**, 4426.
[30] a) S. Bruni, F. Cariati, A. Dei, D. Gatteschi, *Inorg. Chim. Acta* **1991**, *186*, 157; b) A. Dei, D. Gatteschi, L. Pardi, *Inorg. Chem.* **1990**, *29*, 1442.
[31] a) K. C. Fortner, J. P. Bigi, S. N. Brown, *Inorg. Chem.* **2005**, *44*, 2803; b) P. Gupta, A. Das, F. Basuli, A. Castineiras, W. S. Sheldrick, H. Mayer-Figge, S. Bhattacharya, *Inorg. Chem.* **2005**, *44*, 2081; c) C. Carbonera, A. Dei, J.-F. Letard, C. Sangregorio, L. Sorace, *Angew. Chem.* **2004**, *116*, 3198; *Angew. Chem. Int. Ed.* **2004**, *43*, 3136; d) T.-T. Luo, Y.-H. Liu, H.-L. Tsai, C.-C. Su, C.-H. Ueng, K.-L. Lu, *Eur. J. Inorg. Chem.* **2004**, 4253; e) M. Kawahara, Md. K. Kabir, K. Yamada, K. Adachi, H. Kumagai, Y. Narumi, K. Kindo, S. Kitagawa, S. Kawata, *Inorg. Chem.* **2004**, *43*, 92; f) A. Yoshino, H. Matsudaira, E. Asato, M. Koikawa, T. Shiga, M. Ohba, H. Okawa, *Chem. Commun.* **2002**, 1258; g) B. F. Abrahams, J. Coleiro, K. Ha, B. F. Hoskins, S. D. Orchard, R. Robson, *J. Chem. Soc. Dalton Trans.* **2002**, 1586; h) C. Papadimitriou, P. Veltsistas, J. Marek, J. Novosad, A. M. Z. Slawin, J. D. Woollins, *Inorg. Chem. Commun.* **1998**, *1*, 418; i) K. Heinze, G. Huttner, L. Zsolnai, A. Jacobi, P. Schober, *Chem. Eur. J.* **1997**, *3*, 732; j) S. Kawata, S. Kitagawa, M. Kondo, I. Furuchi, M. Manakata, *Angew. Chem.* **1994**, *106*, 1851; *Angew. Chem. Int. Ed. Engl.* **1994**, *33*, 1759; k) F. Lloret, M. Julve, J. Faus, X. Solans, Y. Journaux, I. Morgenstern-Badarau, *Inorg. Chem.* **1990**, *29*, 2232; l) S. Liu, S. N. Shaikh, J. Zubieta, *Inorg. Chem.* **1989**, *28*, 723; m) S. Liu, S. N. Shaikh, J. Zubieta, *Inorg. Chem.* **1988**, *27*, 3064; n) J. V. Folgado, R. Ibanez, E. Coronado, D. Beltran, J. M. Savariault, J. Galy, *Inorg. Chem.* **1988**, *27*, 19; o) P. E. Riley, S. F. Haddad, K. N. Raymond, *Inorg. Chem.* **1983**, *22*, 3090; p) C. A. Tsipis, M. P. Sigalas, V. P. Papageorgiou, M. N. Bakola-Christianopoulou, *Can. J. Chem.* **1983**, *61*, 1500; q) J. Kuyper, *Inorg. Chem.* **1979**, *18*, 1484; r) J. T. Wrobleski, D. B. Brown, *Inorg. Chem.* **1979**, *18*, 498; s) C. G. Pierpont, L. C. Francesconi, D. N. Hendrickson, *Inorg. Chem.* **1978**, *17*, 3470; t) A. M. Talati, V. N. Mistry, *Mater. Sci. Eng.* **1972**, *10*, 287; u) K. S. Min, A. G. DiPasquale, J. A. Golen, A. L. Rheingold, J. S. Miller, *J. Am. Chem. Soc.* **2007**, *129* , 2360; v) K. S. Min, A. L. Rheingold, A. DiPasquale, J. S. Miller, *Inorg. Chem.* **2006**, *45*, 6135.
[32] a) S. Ghumaan, B. Sarkar, S. Patra, K. Parimal, J. van Slageren, J. Fiedler, W. Kaim, G. K. Lahiri, *Dalton Trans.* **2005**, 706; b) A. Nayak, S. Patra, B. Sarkar, S. Ghumaan, V. G. Puranik, W. Kaim, G. K. Lahiri, *Polyhedron* **2005**, *24*, 333.
[33] J. A. Zampese, F. R. Keene, P. J. Steel, *Dalton Trans.* **2004**, 4124.
[34] T. Koiwa, Y. Masuda, J. Shono, Y. Kawamoto, Y. Hoshino, T. Hashimoto, K. Natarajan, K. Shimizu, *Inorg. Chem.* **2004**, *43*, 6215.
[35] a) T. Hashimoto, S. Hara, Y. Shiraishi, Mayumi, K. Natarajan, K. Shimizu, *Inorg. Chim. Acta* **2005**, *358*, 2207; b) D. R. Eaton, *J. Am. Chem. Soc.* **1965**, *87*, 3097.
[36] a) N. Bag, G. K. Lahiri, P. Basu, A. Chakravorty, *J. Chem. Soc. Dalton Trans.* **1992**, 113; b) N. Bag, A. Pramanik, G. K. Lahiri, A. Chakravorty, *Inorg. Chem.* **1992**, *31*, 40.
[37] a) G. K. J. Chao, R. L. Sime, R. J. Sime, *Acta. Crystallogr. Sect. B* **1973**, *29*, 2845; b) S. Maji, B. Sarkar, S. Patra, J. Fiedler, S. M. Mobin, V. G. Puranik, W. Kaim, G. K. Lahiri, *Inorg. Chem.* **2006**, *45*, 1316; c) E. Melendez, V. Lopez, T. Concolino, A. L. Rheingold, *J. Organomet. Chem.* **2004**, *689*, 3082; d) G. D. Frey, Z. R. Bell, J. C. Jeffery, M. D. Ward, *Polyhedron* **2001**, *20*, 3231; e) E. Melendez, I. Guzei, A. L. Rheingold, *J. Chem. Crystallogr.* **1999**, *29*, 399; f) T. Hashimoto, A. Endo, N. Nagao, G. P. Sato, K. Natarajan, K. Shimizu, *Inorg. Chem.* **1998**, *37*, 5211; g) P. A. Reynolds, J. W. Cable, A. N. Sobolev, B. N. Figgis, *J. Chem. Soc. Dalton Trans.* **1998**, 559; h) K. Mashima, H. Fukumoto, K. Tani, M. Haga, A. Nakamura, *Organometallics* **1998**, *17*, 410; i) M. A. Bennett, H. Neumann, A. C. Willis, V. Ballantini, P. Pertici, B. E. Mann, *Organometallics* **1997**, *16*, 2868; j) E. Melendez, R. Ilarraza, G. P. A. Yap, A. L. Rheingold, *J. Organomet. Chem.* **1996**, *522*, 1; k) T. S. Knowles, M. E. Howells, B. J. Howlin, G. W. Smith, C. A. Amodio, *Polyhedron* **1994**, *13*, 2197; l) R. Schneider, T. Weyhermueller, K. Wieghardt, B. Nuber, *Inorg. Chem.* **1993**, *32*, 4925; m) R. Schneider, K. Wieghardt, B. Nuber, *Inorg. Chem.* **1993**, *32*, 4935; n) H. Matsuzawa, Y. Ohashi, Y. Kaizu, H. Kobayashi, *Inorg. Chem.* **1988**, *27*, 2981; o) S. Aynetchi, P. B. Hitchcock, E. A. Seddon, K. R. Seddon, Y. Z. Yousif, J. A. Zora, K. Stuckey, *Inorg. Chim. Acta* **1986**, *113*, L7–L9.
[38] R. L. Carlin, *Magnetochemistry*, Springer, Berlin, **1986**, p. 14.
[39] a) Z. Shen, J.-L. Zou, S. Gao, Y. Song, C.-M. Che, H.-K. Fun, X.-Z. You, *Angew. Chem.* **2000**, *112*, 3779; *Angew. Chem. Int. Ed.* **2000**, *39*, 3633; b) J. Androulakis, N. Katsarakis, J. Giapintzakis, *Phys. Rev. B* **2001**, *64*, 174401.
[40] O. Kahn, *Molecular Magnetism*, Wiley-VCH, Weinheim, **1993**, p. 107.
[41] S. Patra, B. Sarkar, S. Maji, J. Fiedler, F. A. Urbanos, R. Jiménez-Aparicio, W. Kaim, G. K. Lahiri, *Chem. Eur. J.* **2005**, *11*, 489.
[42] M. C. Barral, R. Gonzalez-Prieto, R. Jiménez-Aparicio, J. L. Priego, M. A. Torres, F. A. Urbanos, *Eur. J. Inorg. Chem.* **2003**, 2339.
[43] F. E. Mabs, D. J. Machin, *Magnetism and Transition Metal Complexes*, Chapman and Hall, London, **1973**, p. 78.
[44] S. Kar, N. Chanda, S. M. Mobin, F. A. Urbanos, M. Niemeyer, V. G. Puranik, R. Jimenez-Aparicio, G. K. Lahiri, *Inorg. Chem.* **2005**, *44*, 1571.
[45] C. Creutz, *Prog. Inorg. Chem.* **1983**, *30*, 1.
[46] a) N. S. Hush, *Coord. Chem. Rev.* **1985**, *64*, 135; b) N. S. Hush, *Prog. Inorg. Chem.* **1967**, *8*, 391.
[47] T. Kobayashi, Y. Nishina, K. Shimizu, G. P. Satô, *Chem. Lett.* **1988**, 1137.
[48] M. Krejcik, M. Danek, F. Hartl, *J. Electroanal. Chem. Interfacial Electrochem.* **1991**, *317*, 179.
[49] W. Kaim, S. Ernst, V. Kasack, *J. Am. Chem. Soc.* **1990**, *112*, 173.
[50] SHELXTL PC 5.03, Siemens Analytical X-ray Instruments Inc., Madison, WI, **1994**.
[51] G. M. Sheldrick, Program for Crystal Structure Solution and Refinement, Universität Göttingen, Göttingen (Germany), **1997**.

Received: May 22, 2008
Revised: July 28, 2008
Published online: October 16, 2008

